

UNIVERSITY OF  
CALIFORNIA  
*Ernest O. Lawrence*  
**Radiation  
Laboratory**

TWO-WEEK LOAN COPY

This is a Library Circulating Copy  
which may be borrowed for two weeks.  
For a personal retention copy, call  
Tech. Info. Division, Ext. 5545

BERKELEY, CALIFORNIA

[illegible]

~~SECRET~~  
**UNCLASSIFIED**

UCRL-868  
Chemistry-Transuranic Elements

UNIVERSITY OF CALIFORNIA

Radiation Laboratory

~~OFFICIAL USE ONLY~~

Contract No. W-7405-eng-48

**UNCLASSIFIED**

Classification change to

by authority of

*R K Wakerling*

By

*B Fickett*

Date

*6-22-56*

Person making change

HIGH ENERGY EXCITATION FUNCTIONS IN THE HEAVY REGION

W. W. Meinke, G. C. Wick, and G. T. Seaborg

September 26, 1950

CAUTION

~~This document contains information affecting the National Defense of the United States. Its transmission or the disclosure of its contents in any manner to an unauthorized person is prohibited and may result in severe criminal penalties under applicable Federal laws.~~

Berkeley, California

UNCLASSIFIED

~~SECRET~~

UCRL-868  
Chemistry-Transuranic Elements  
Page 2

~~OFFICIAL USE ONLY~~

<u>Standard Distribution: Series A</u>	<u>Copy Numbers</u>
Argonne National Laboratory	1-10
Atomic Energy Commission, Washington	11-12
Brookhaven National Laboratory	13-16
Carbide & Carbon Chemicals Division (K-25 Plant)	17-18
Carbide & Carbon Chemicals Division (Y-12 Plant)	19
General Electric Company, Richland	20-25
Hanford Operations Office	26
Iowa State College	27
Kellex Corporation	28
Knolls Atomic Power Laboratory	29-32
Los Alamos	33-35
Mound Laboratory	36-38
Naval Radiological Defense Laboratory	39
NEPA Project	40
New York Operations Office	41-42
Oak Ridge National Laboratory	43-48
Patent Branch, Washington	49
Technical Information Division, ORE	50-64
UCLA Medical Research Laboratory (Warren)	65
University of California Radiation Laboratory	66-68
University of Rochester	69-70
Total	70

INFORMATION DIVISION  
Radiation Laboratory  
Univ. of California  
Berkeley, California

~~SECRET~~

HIGH ENERGY EXCITATION FUNCTIONS IN THE HEAVY REGION

W. W. Meinke,\* G. C. Wick, and G. T. Seaborg  
Radiation Laboratory, Department of Physics,  
and Department of Chemistry  
University of California  
Berkeley, California  
September 26, 1950

ABSTRACT

The electrostatically deflected beam of the 184-inch cyclotron has been used with the stacked foil and absorber technique to determine the excitation functions for the following reactions:  $\text{Th}^{232}(\text{p}, 6\text{n})\text{Pa}^{227}$ ,  $\text{Th}^{232}(\text{p}, 3\text{n})\text{Pa}^{230}$ ,  $\text{Th}^{232}(\text{d}, 7\text{n})\text{Pa}^{227}$ ,  $\text{Th}^{232}(\alpha, \text{p}8\text{n})\text{Pa}^{227}$ ,  $\text{Th}^{232}(\alpha, \text{p}5\text{n})\text{Pa}^{230}$ , and  $\text{U}^{238}(\text{p}, \alpha 8\text{n})\text{Pa}^{227}$ . The data are presented graphically and discussed individually for each of the reactions. Some rough excitation function data have also been determined for the reactions  $\text{Th}^{232}(\text{d}, 4\text{n})\text{Pa}^{230}$ ,  $\text{U}^{238}(\text{p}, \alpha 5\text{n})\text{Pa}^{230}$ ,  $\text{Th}^{232}(\alpha, 7\text{n})\text{U}^{229}$ , and  $\text{Th}^{232}(\alpha, 6\text{n})\text{U}^{230}$ . The results are discussed in terms of compound nucleus formation, transparency effects, and other factors in order to arrive at a qualitative picture for the mechanism of high energy nuclear reactions with heavy nuclei.

---

\*Present address: Department of Chemistry, University of Michigan,  
Ann Arbor, Michigan.

## HIGH ENERGY EXCITATION FUNCTIONS IN THE HEAVY REGION

W. W. Meinke, G. C. Wick, and G. T. Seaborg  
Radiation Laboratory, Department of Physics,  
and Department of Chemistry  
University of California  
Berkeley, California

## I. INTRODUCTION

In the past, investigations of excitation functions with the bombarding particles from relatively low energy accelerators<sup>1</sup> have led to a better understanding of low energy nuclear reactions. Many precise measurements have been made in this study of the dependency of reaction yield upon bombardment energy.

The availability of high energy particles makes it possible to extend this method of investigation to the energy region which is well beyond that of the binding energy of the individual nucleons. Excitation functions of a few light element reactions with high energy particles have been reported,<sup>2</sup> but those of heavy elements have not been investigated except for one determination by E. L. Kelly on the  $\text{Bi}^{209}(\alpha, 2n)\text{At}^{211}$  reaction.<sup>3</sup>

During the course of work on the artificial collateral series<sup>4,5</sup> produced in bombardments of thorium with deuterons and helium ions from the 184-inch

---

<sup>1</sup>See, for example, E. T. Clarke and J. W. Irvine, Jr., Phys. Rev. 69, 680 (1946); E. L. Kelly and E. Segrè, Phys. Rev. 75, 999 (1949); see also Appendix.

<sup>2</sup>See: A. C. Helmholtz and J. W. Peterson, Phys. Rev. 73, 541 (1948) abstr.; R. L. Thornton and R. W. Senseman, Phys. Rev. 72, 872 (1947); R. W. Chupp and E. M. McMillan, Phys. Rev. 72, 873 (1947); Bockhop, Helmholtz, Softky, Rose, and Breakey, Phys. Rev. 75, 1469 (1949) abstr.

<sup>3</sup>E. L. Kelly, University of California Radiation Laboratory Report UCRL-277 (Jan., 1949).

<sup>4</sup>Ghiorso, Meinke, and Seaborg, Phys. Rev. 74, 695 (1948).

<sup>5</sup>Ibid., 75, 314 (1949).

cyclotron of the University of California Radiation Laboratory, we became interested in determining, through excitation functions, the energies for maximum yield of certain nuclides produced by spallation reactions. These preliminary experiments seemed to indicate that the transparency effect discussed by Serber<sup>6</sup> is important in spallation reactions involving the heavy elements. It was also apparent from these early experiments that there is a definite trend toward lower absolute yields as more neutrons are expelled in the reaction leading to the product isotope.

In view of the value which excitation functions for heavy elements would have toward giving data to help in the understanding of high energy nuclear reactions, and also because of the relative ease with which the yield of the alpha-emitting product nuclides can be quantitatively determined, it was decided to undertake the measurement of a number of such excitation functions. Included among the reactions which lend themselves to investigation are those in which large numbers of neutrons are emitted, such as the (p,6n) and (d,7n) reactions, and reactions in which charged particles are emitted together with neutrons, so that it seemed possible to study in some detail the interplay between compound nucleus formation and transparency effects at relatively high energies.

## II. PROCEDURE

Stacked foils of 5-mil thorium (or uranium) metal with varying thicknesses of copper metal sandwiched between were bombarded with charged particles in the electrostatically deflected beam of the 184-inch frequency-modulated cyclotron. The first weighed foil intercepted the nearly full energy particles from the cyclotron (348-Mev protons, 194-Mev deuterons, or 388-Mev helium ions) and successive foils were struck by particles of decreasing energy until the entire

---

<sup>6</sup>R. Serber, Phys. Rev. 72, 1114 (1947).

beam energy had been expended in the foil stack. The energy of particles impinging on any one foil was determined by the use of range-energy relationships between the absorbing material and the particles.<sup>7,8</sup> Since the decrease in energy of the high energy particles in passing through each 5-mil foil is relatively small, the yields from such foils placed at selected points in a stack of copper absorbers define rather well a thin target (differential) excitation function.

In each case sixteen foils were placed at known energy positions in the stack. After bombardment the 0.4-gram thorium (or 0.7-gram uranium) foils were removed and dissolved in portions of concentrated nitric acid (with ammonium fluosilicate in the case of thorium). The 38.3-min.  $\text{Pa}^{227}$  and the 17-day  $\text{Pa}^{230}$  isotopes are well suited for separation and characterization as reaction products. The element protactinium is very easily and cleanly separated chemically from all other alpha-emitters produced in the bombardments. This simple protactinium chemistry also lends itself to a mass production scheme which makes it possible to work up and have ready to count 16 bombarded thorium samples in a short time (less than two hours). In the cases in which protactinium isotopes were to be measured, a protactinium fraction was separated by a solvent extraction procedure involving simultaneous equilibration of the nitric acid solution of each sample with a solution of thenoyltrifluoroacetone<sup>9</sup> (TTA) in benzene.

---

<sup>7</sup>Aron, Hoffman, and Williams, University of California Radiation Laboratory Report UCRL-121, 1st and 2nd revisions (1948, 1949); former also issued as U. S. Atomic Energy Commission Unclassified Document AECU-103 (Nov., 1948).

<sup>8</sup>These range-energy values and the experimental yield for each absorber position, as obtained in this work, are presented in detail in the Ph.D. thesis of W. Wayne Meinke, University of California (Jan., 1950).

<sup>9</sup>J. C. Reid and M. Calvin, U. S. Atomic Energy Commission Declassified Document MDDC-1405 (Aug., 1947); also, J. Am. Chem. Soc. 72, 2948 (1950).



The protactinium was thus extracted as a complex ion into the organic layer which was evaporated and flamed on thin, 1-inch diameter platinum plates.

The alpha-particle activity was counted in a standard argon-filled ionization chamber in which the pulses from the electron collection were fed through a fast amplifier into a scale of 512 counting circuit. When it was necessary to count beta-particles, an end window, alcohol-quenched, argon-filled Geiger counter tube with a mica window ( $\sim 3 \text{ mg/cm}^2$ ) was used in conjunction with a scale of 64 counting circuit.

Immediately after bombardment and usually for about five hours thereafter the 38.3-min. isotope  $\text{Pa}^{227}$  and its daughters present the predominant alpha-activity in the pure protactinium chemical fractions. After a period of several weeks, the only prominent alpha-activity is due to the  $\text{U}^{230}$  series growing from the  $\text{Pa}^{230}$  isotope. The radioactive purity of these samples was checked by alpha-particle decay measurements indicating the 38.3-min. decay of the  $\text{Pa}^{227}$ , and, after other protactinium isotopes had decayed out, by alpha-particle pulse analysis for the  $\text{U}^{230}$  series. A 48-channel alpha-particle pulse analyzer<sup>10</sup> equipped with a fast sample changing mechanism was used for the latter measurements. The observed counting rates were corrected for decay or daughter growth, target weight, etc., converted to disintegrations per minute at the end of bombardment, and plotted against the bombarding energy for each sample, thus giving the excitation function for the particular reaction studied.

Absolute chemical yields were not determined, but since all samples in a run were worked up simultaneously with the same chemical procedure used on each sample, the relative chemical yields are accurate to within about five percent.

---

<sup>10</sup>See: Ghiorso, Jaffey, Robinson, and Weissbourd, National Nuclear Energy Series, Plutonium Project Record, Vol. 14B, "The Transuranium Elements: Research Papers," Paper No. ~~17-3~~<sup>16-8</sup> (McGraw-Hill Book Co., Inc., New York, 1949).

The calculated energy values used for these excitation functions are only approximate, particularly at the lower end of the energy scale, because of beam straggling and the spread in initial energy of the particles in the 184-inch cyclotron as discussed more fully later. Consequently, while maximum yield and threshold energy values observed from the experimental curves may be considerably in error on the absolute energy scale, they should be significant when considered in relation to the rest of the excitation function curve.

The experimental techniques used in the work are discussed more thoroughly in a later section (Section V).

### III. RESULTS

Excitation functions were obtained for the (p,6n) and (p,3n) reactions on thorium, the (p, $\alpha$ 8n) and (p, $\alpha$ 5n) reactions on uranium, the (d,7n) and (d,4n) reactions on thorium, and the ( $\alpha$ ,p8n) and ( $\alpha$ ,p5n) reactions on thorium as well as rough data for some ( $\alpha$ ,xn) reactions on thorium. The bombardments were usually of about 90-minutes duration and the plotted disintegration rates are corrected for decay back to the end of the bombardment. Usually at least two runs were made for each reaction. The data are presented graphically for most cases and discussed individually for each of the reactions in the following sections. The yields below the thresholds are due to the fact that a few particles of high energy reach the target by coming in through the side of the stack of absorber foils.

#### A. Protons

1.  $\text{Th}^{232}(\text{p},6\text{n})\text{Pa}^{227}$ .— The results of two different bombardments in which this reaction was studied are plotted in Fig. 1. The points fall on a smooth curve whose maximum rises a factor of almost 20 above the yield value at full energy (348 Mev). The range of the protons is sufficiently great to make necessary

Fig. 1. Excitation function for the  $\text{Th}^{232}(\text{p}, 6\text{n})\text{Pa}^{227}$  reaction. Circles represent Run I; crosses, Run II. (The apparent yield below the threshold energy shown in this and following figures is due to a small fraction of the incident beam striking the stack of foils from the side.)

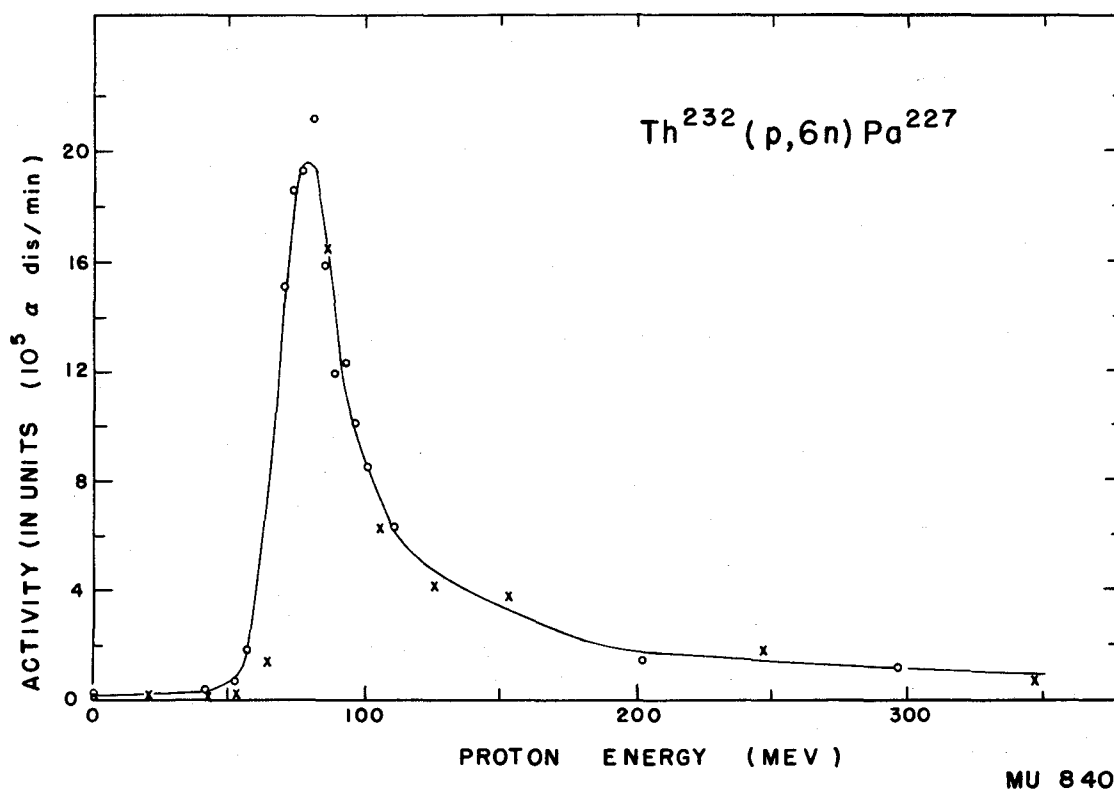


Fig. 1

the proper corrections for nuclear absorption and these have been made as described later (Section V-B). The curve is not drawn through the point at 81 Mev even though this point would appear to be at the peak of the excitation function. When counted later for  $U^{230}$ , this sample gave a yield value which was definitely displaced from the curve for the (p,3n) reaction (see Fig. 3). Possibly some error in aliquot measurements caused the discrepancy. In Fig. 2 the peak of the curve is plotted on an enlarged scale to show the extent of the symmetry involved. It can be seen that on the high energy side of the peak another mode of reaction becomes apparent and is superimposed on a somewhat symmetrical peak.

A single experiment in which the collimated external proton beam was used gave a value of about  $2.5 \times 10^{-3}$  barns as the absolute cross section for this reaction at full energy (348 Mev). The experimental details are given later. From this cross section value we see that the cross section at the peak of the curve should be about  $5 \times 10^{-2}$  barns. Because of the questionable chemical yield discussed later on, this can only be considered the maximum value for the cross section, further experiments being necessary to establish the true value. It may be pointed out that the measured cross section at the peak is lower than the true maximum cross section, because of the energy spread effect. The discussion in section V-B, however, shows that the correction involved is not large. Similarly small corrections apply also to the peak cross sections mentioned later.

2.  $Th^{232}(p,3n)Pa^{230}$ .-- The yield values for the reaction  $Th^{232}(p,3n)Pa^{230}$  are plotted in Fig. 3. Here again a factor of about 20 between the maximum yield and the yield at full energy is found.

A very interesting observation can be made from the curves for the (p,6n) and (p,3n) reactions on thorium. Although the curves for the two reactions have a similar shape and a comparable ratio of peak yield to full energy yield, there is a difference in absolute yield of about five between the two in favor of the (p,3n) reaction. This difference was found by determination of the number of atoms formed by each reaction at the peak of the excitation function. The ratios

Fig. 2. Excitation function for the  $\text{Th}^{232}(\text{p}, 6\text{n})\text{Pa}^{227}$  reaction on enlarged scale. Circles represent Run I; crosses, Run II. Absolute value of energy scale not accurate (see text).

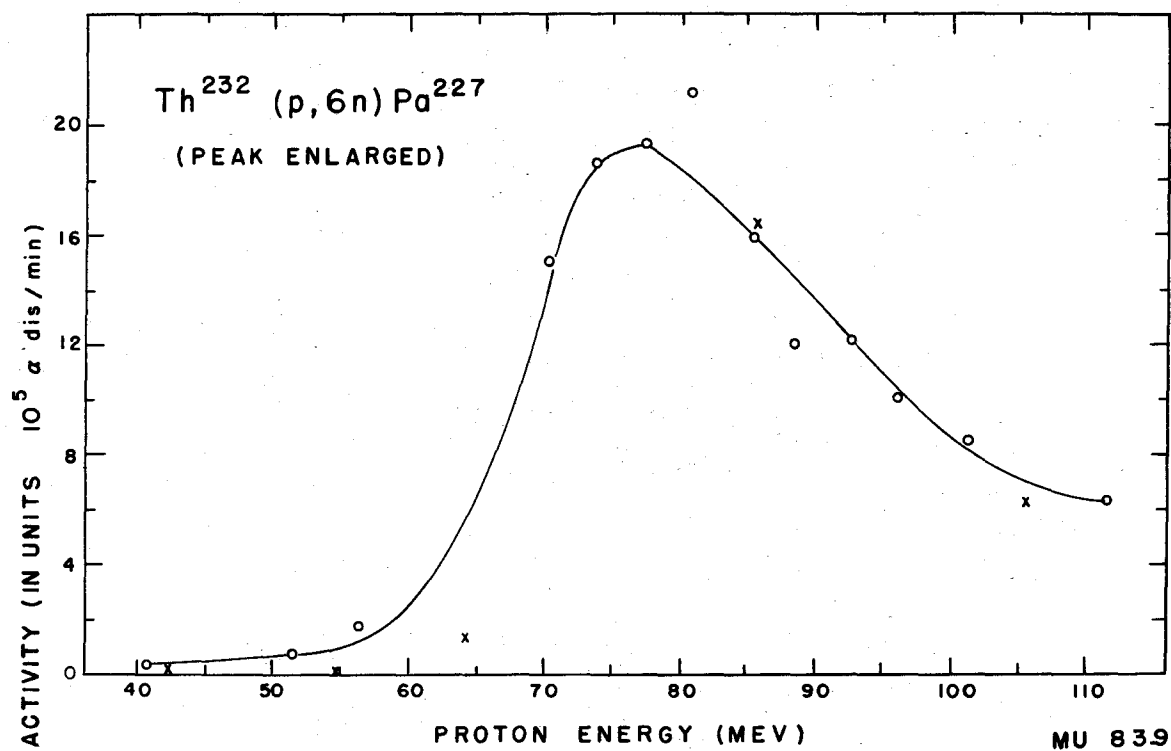


Fig. 2

Fig. 3. Excitation function for the  $\text{Th}^{232}(\text{p}, 3\text{n})\text{Pa}^{230}$  reaction. Circles represent Run I; crosses, Run II.



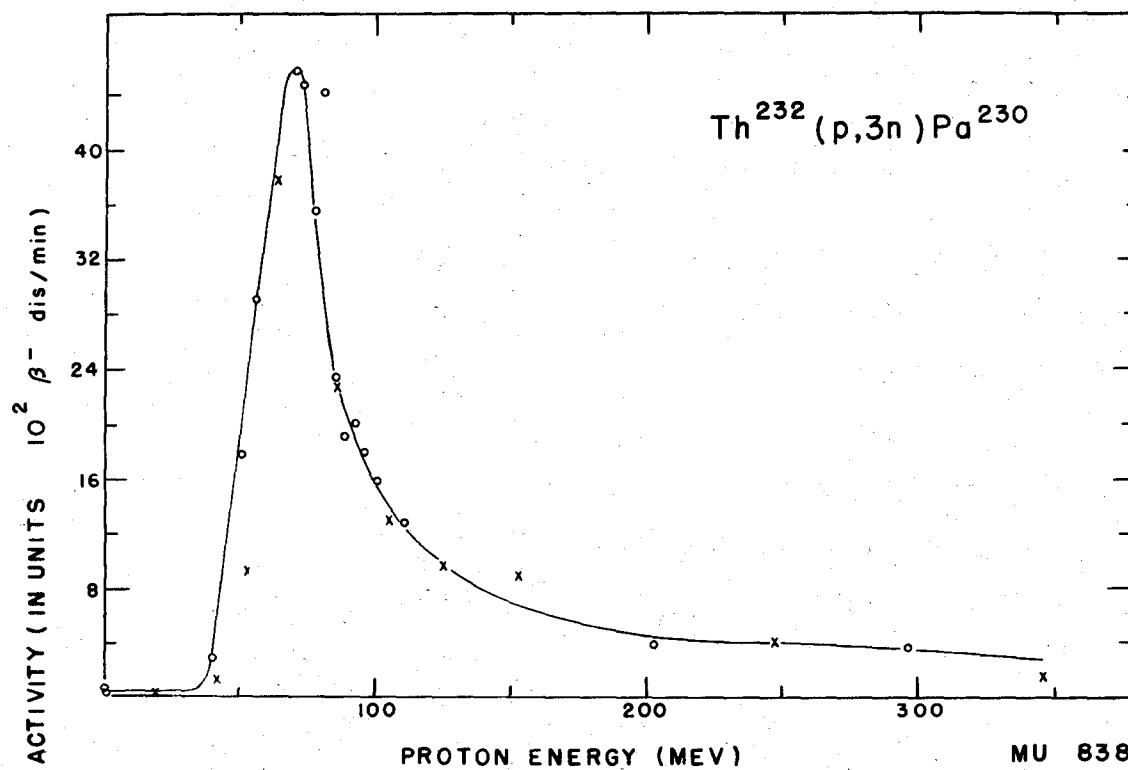


Fig. 3

of about ten percent beta-decay branching<sup>11</sup> for  $\text{Pa}^{230}$  and about 85 percent alpha-decay branching<sup>4</sup> for  $\text{Pa}^{227}$  were considered in the calculations. By using this factor of five and the yield mentioned in the previous section, it follows that at the peak of its excitation function, the absolute cross section for the (p,3n) reaction is about 0.25 barns.

3.  $\text{U}^{238}(\text{p},\alpha 8\text{n})\text{Pa}^{227}$ .-- In addition to the thorium bombardments, the protactinium fraction was separated from pieces of 5-mil uranium foil, bombarded under the same conditions as the thorium foil. The results of these uranium bombardments are given in Fig. 4. Considerable trouble was encountered in the attempts to develop chemical procedures which would give consistent chemical yields for all of the 16 foils in a bombardment. This trouble is reflected in the somewhat larger scattering of yield values for this reaction than for the reactions in thorium bombardments. Despite the scattering, however, the points do define a very broad peak near the high energy portion of the curve.

4.  $\text{U}^{238}(\text{p},\alpha 5\text{n})\text{Pa}^{230}$ .-- Too little activity was available from the reaction  $\text{U}^{238}(\text{p},\alpha 5\text{n})\text{Pa}^{230}$  to make it feasible to obtain a definitive yield curve. The points obtained scattered much more than for the above reaction but did define a broad peak which was near the high energy portion of the curve but displaced somewhat to the low energy side of the (p, $\alpha 8\text{n}$ ) curve. The ratio of yields for the two reactions at the peaks of their excitation functions is about six or seven in favor of the (p, $\alpha 5\text{n}$ ) reaction.

#### B. Deuterons

In the (d,xn) reactions, as in the (p,xn) reactions, excitation functions with definite sharp peaks are found, even when as many as seven neutrons are emitted. The range of full energy deuterons (194 Mev) from the 184-inch cyclotron

---

<sup>11</sup>M. H. Studier and R. J. Bruehlman, as listed by G. T. Seaborg and I. Perlman, Rev. Mod. Phys. 20, 585 (1948).

Fig. 4. Excitation function for the  $U^{238}(p,\alpha 8n)Pa^{227}$  reaction. Circles represent Run I; crosses, Run II; and deltas, part of Run III.

MU 843

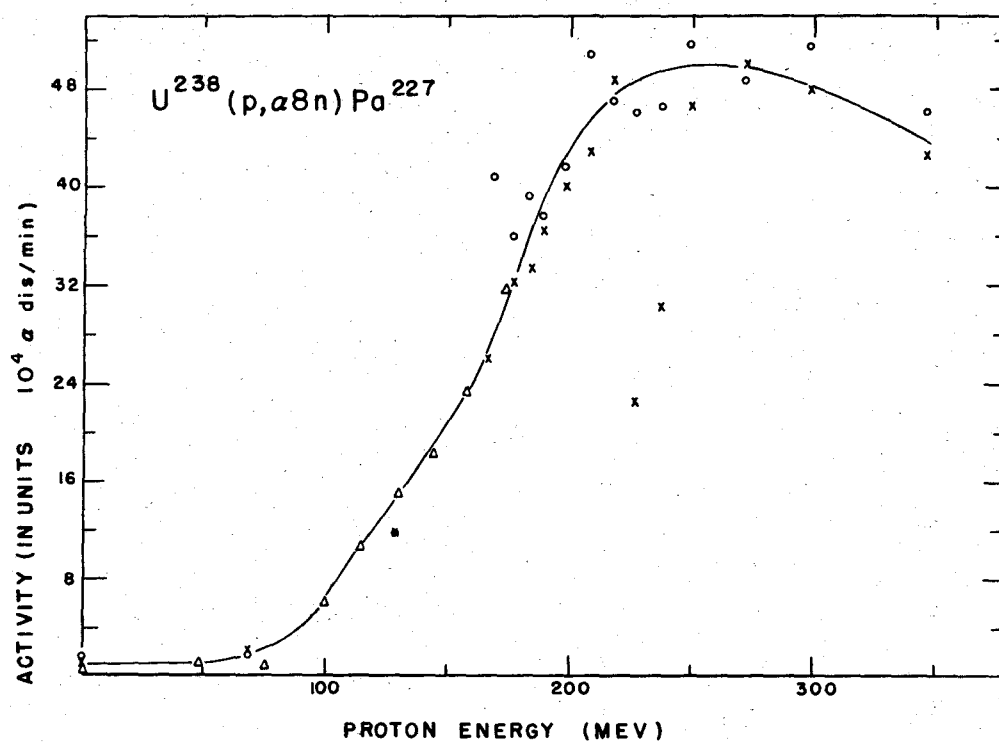


Fig. 4

is about 2.5 cm in copper, and although the nuclear absorption has not been measured, the corrections would certainly be less than those made in the proton bombardments. The total beam current available with the deuteron beam of the large cyclotron is roughly equal to that of the proton beam.

1.  $\text{Th}^{232}(\text{d},7\text{n})\text{Pa}^{227}$ .-- The yields for the reaction  $\text{Th}^{232}(\text{d},7\text{n})\text{Pa}^{227}$  are plotted in Fig. 5. The reaction yield curve rises to a very definite peak which represents about eight times the yield value at full energy. An enlarged plot of the peak of this excitation curve is shown in Fig. 6. Using the same methods as for the  $(\text{p},6\text{n})$  reaction, absolute cross section determinations for this reaction were made. The average of values obtained with full energy deuterons is  $2.3 \times 10^{-3}$  barns, making the cross section at the peak of the curve about  $1.8 \times 10^{-2}$  barns. These values are probably accurate to within 15 percent.

2.  $\text{Th}^{232}(\text{d},4\text{n})\text{Pa}^{230}$ .-- In these thorium bombardments unfortunately, the energy values which were chosen so as to obtain an outline of the peak for the  $(\text{d},7\text{n})$  excitation function, are not suitable to outline completely the peak of the curve for the reaction  $\text{Th}^{232}(\text{d},4\text{n})\text{Pa}^{230}$ . The position of the points makes it possible to observe only the high energy slope of this peak. From these experimental points, however, we can set a lower limit of about four for the ratio of total atoms  $\text{Pa}^{230}/\text{Pa}^{227}$  formed at the peaks of the yield functions.

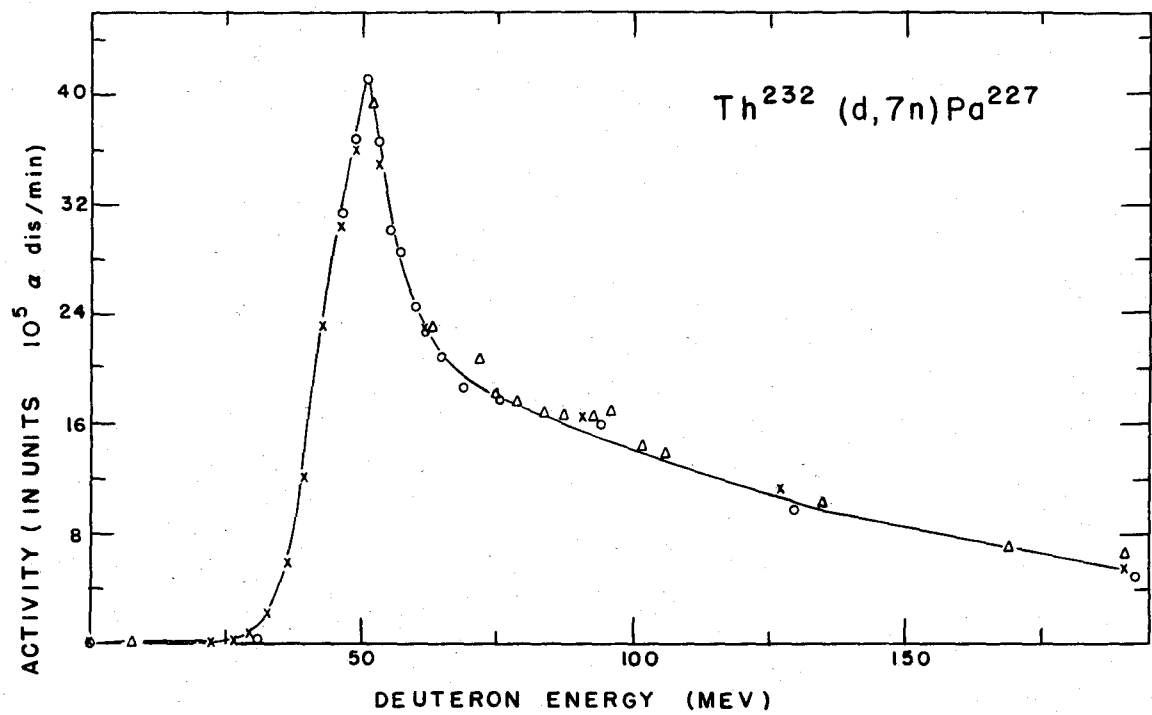
3.  $\text{Th}^{232}(\text{d},7\text{n})\text{Pa}^{227}$ ,  $\text{Al}^{27}(\text{d},\text{ap})\text{Na}^{24}$ , and  $\text{C}^{12}(\text{d},\text{n})\text{N}^{13}$ .-- In an effort to determine more accurately the threshold energy for the  $(\text{d},7\text{n})$  reaction on thorium, simultaneous bombardment of thorium, aluminum, and carbon (as polystyrene) foils was attempted. The excitation functions for the  $(\text{d},\text{ap})$  reaction on aluminum<sup>12</sup> and the  $(\text{d},\text{n})$  reaction on carbon<sup>13</sup> had been previously studied at low energies and it was thought that the determination of the threshold values for these

---

<sup>12</sup>E. T. Clarke, Phys. Rev. 71, 187 (1947).

<sup>13</sup>H. W. Newson, Phys. Rev. 51, 620 (1937).

Fig. 5. Excitation function for the  $\text{Th}^{232}(\text{d}, 7\text{n})\text{Pa}^{227}$  reaction. Circles represent Run I; crosses, Run II; and deltas, Run III.

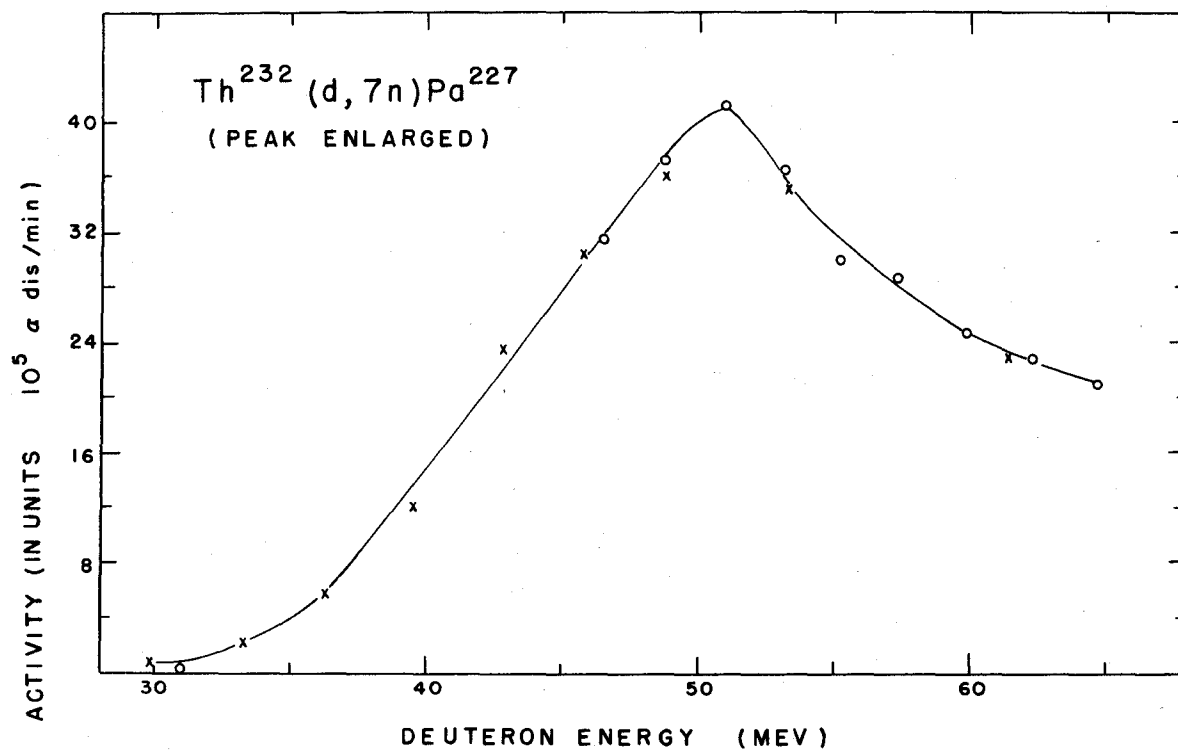


MU 844

Fig. 5

Fig. 6. Excitation function for the  $\text{Th}^{232}(\text{d}, 7\text{n})\text{Pa}^{227}$  reaction on enlarged scale. Circles represent Run I; and crosses, Run II. Absolute value of energy scale not accurate (see text).





MU 841

Fig. 6

reactions in stacked foils in the 184-inch cyclotron might establish a low energy anchor point for the excitation function energy scale. Fig. 7 presents the results of the simultaneous determination of these three excitation functions from a bombardment of one hour and forty-five minutes duration. In this case the abscissae are given in thickness of aluminum absorber rather than energy because of the uncertainty of the latter near the end of the range of the deuterons. Chemical separations were not needed in the case of the aluminum and polystyrene targets.

Unfortunately, straggling and the initial energy distribution of the deuteron beam makes an exact interpretation of these experimental threshold values difficult. It can only be said that the difference in threshold between the  $C^{12}(d,n)N^{13}$  reaction (which occurs at about 2 Mev) and that of the reaction  $Th^{232}(d,7n)Pa^{227}$  amounts to about 1200 mg/cm<sup>2</sup> of aluminum for the range of the deuteron, which corresponds<sup>7</sup> very roughly to an energy of about 40 Mev for the threshold of the latter reaction.

### C. Helium Ions

The determination of excitation functions from bombardments with helium ions is more difficult since the beam current in the 184-inch cyclotron is only about one-tenth that obtained for protons and deuterons. In addition, for all reactions other than the  $(\alpha, xn)$  reactions, there is the possibility that deuteron contamination of the helium-ion beam can produce the activity in question by another more favorable reaction and consequently obscure the yield of the reaction under study. The  $(\alpha, pxn)$  reactions producing protactinium isotopes from thorium were studied in bombardments in which a one-half inch stack of copper foils was required to absorb completely the helium-ion beam. A few experiments were also made with the  $(\alpha, xn)$  reactions.

Fig. 7. Excitation functions for the  $\text{Th}^{232}(\text{d}, 7\text{n})\text{Pa}^{227}$ ,  $\text{Al}^{27}(\text{d}, \text{ap})\text{Na}^{24}$ , and  $\text{C}^{12}(\text{d}, \text{n})\text{N}^{13}$  reactions obtained in a single bombardment with 194-Mev deuterons reduced in energy by copper absorbers to 50 Mev (represented as 0  $\text{mg}/\text{cm}^2$  Al).

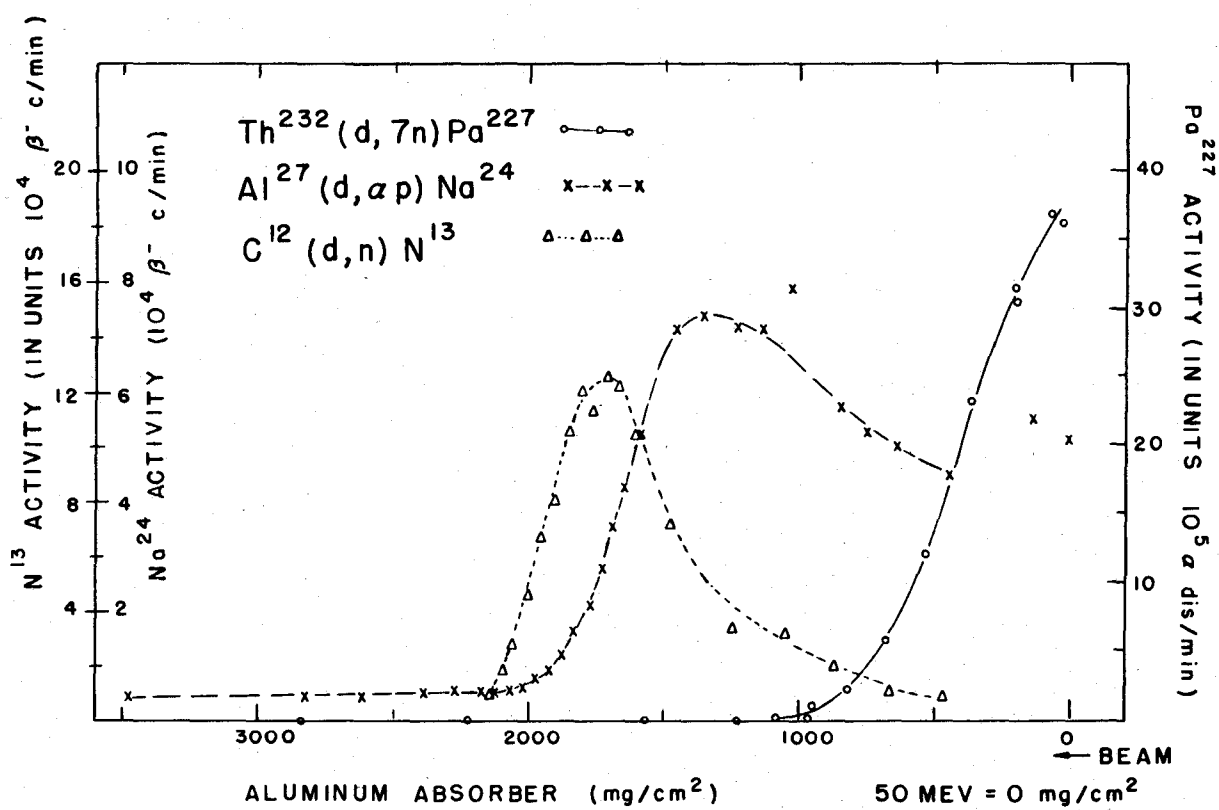


Fig. 7

MU 842

1.  $\text{Th}^{232}(\alpha, p8n)\text{Pa}^{227}$ .— Fig. 8 shows the yield values for  $\text{Pa}^{227}$  obtained from a bombardment of thorium with helium ions. This curve shows no sharp peak.

2.  $\text{Th}^{232}(\alpha, p5n)\text{Pa}^{230}$ .— Fig. 9 shows a companion curve to the one above obtained for the  $(\alpha, p5n)$  reaction in the same bombardment. In these  $(\alpha, pxn)$  curves the peak yield for the  $(\alpha, p5n)$  reaction is greater by a factor of about seven than that for the  $(\alpha, p8n)$  reaction.

3.  $\text{Th}^{232}(\alpha, xn)$  Reactions.— Insufficient 20.8-day  $\text{U}^{230}$  or 58-min.  $\text{U}^{229}$  alpha-activity was formed in bombardments of stacked foils with the electrostatically deflected beam to permit accurate determination of the  $(\alpha, 6n)$  or  $(\alpha, 7n)$  excitation functions. In addition, the chemical procedures required to obtain pure uranium samples from the bombarded material were not adaptable to the mass production methods employed in the protactinium separations. Consequently, the only definitive experiments have been individual bombardments of thorium foils at different radii (and hence different energies) in the internal cyclotron beam without the benefit of a monitor but with conditions of each bombardment as nearly equivalent as possible. These experiments indicate that the  $(\alpha, xn)$  excitation functions exhibit sharp peaks of about the same width as that of the peak in the yield curve for the  $(p, 6n)$  reaction. The shape of the curve beyond the high energy side of the peak has not yet been determined.

#### IV. DISCUSSION

The data presented in the foregoing figures are unfortunately rather rough due to the difficulty of the experimental procedures and more especially to the unavoidable limitations placed by the spread of energy in the particle beams delivered by the 184-inch cyclotron. Nevertheless, they give some interesting and in some cases rather surprising information on the mechanism of nuclear reactions in which relatively large numbers of nucleons are expelled.

Fig. 8. Excitation function for the  $\text{Th}^{232}(\alpha, p8n)\text{Pa}^{227}$   
reaction.

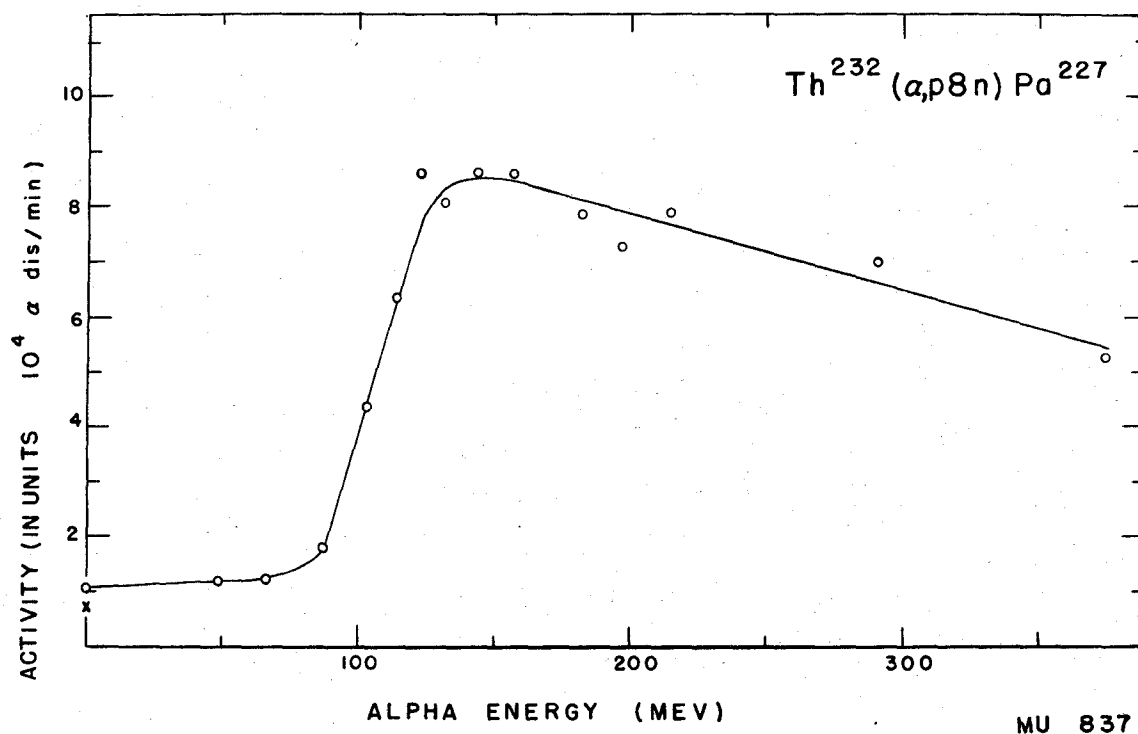
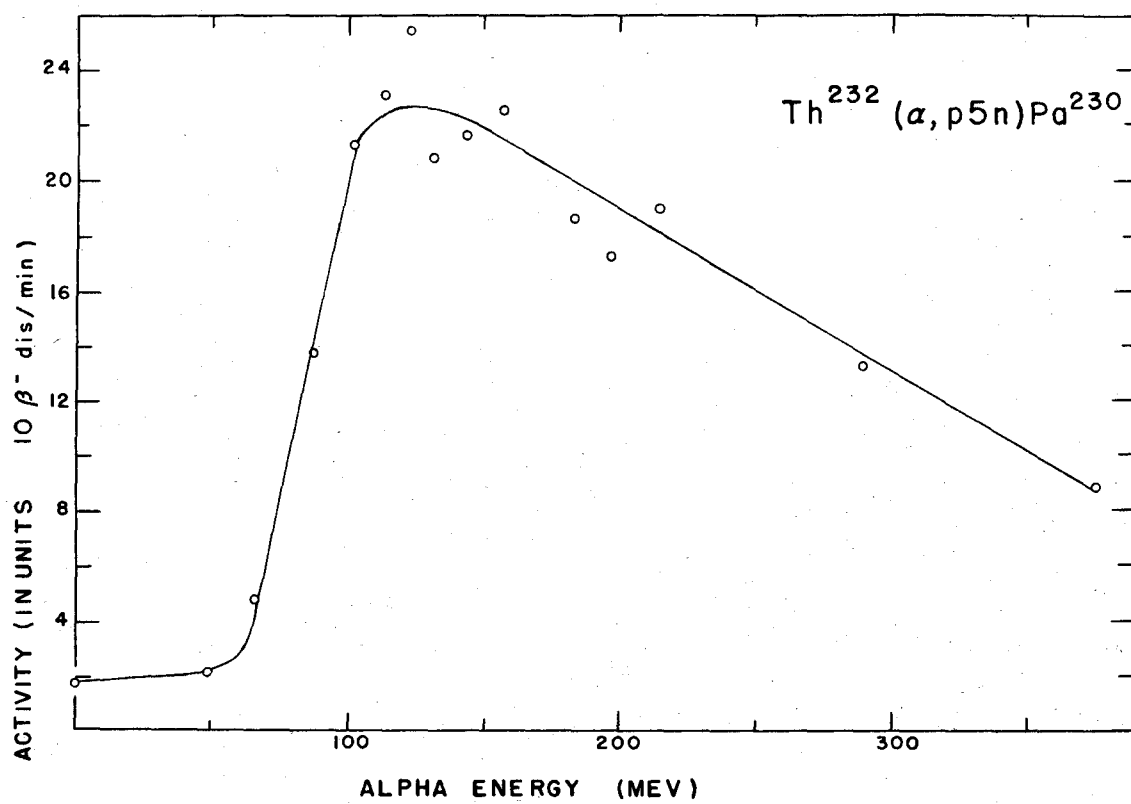


Fig. 8

Fig. 9. Excitation function for the  $\text{Th}^{232}(\alpha, p5n)\text{Pa}^{230}$   
reaction.





MU 845

Fig. 9

Comparable information on such reactions has not been obtained hitherto, and therefore, even rather rough data are of interest.

The excitation function shown in Fig. 1 for the  $(p,6n)$  reaction shows a surprisingly sharp peak. The width at one-half maximum, uncorrected for the spread in energy of the protons, is some 25 Mev and should probably be noticeably less than this if correction could be made for the unknown spread in energy of the initial 348-Mev protons (the possible magnitude of this spread and that due to straggling is discussed briefly further on in Section V-B). This seems to indicate that even at energies as high as some 50 to 75 Mev, the mechanism of reaction involves the formation of a compound nucleus similar to that which forms such a successful model for explaining the course of reactions at lower energies. The sharpness of this peak may be due to the fact that a heavy nucleus is involved and perhaps is not to be expected in the case of the  $(p,6n)$  reaction with much lighter nuclei. The  $(p,3n)$  and the  $(d,7n)$  reactions, presented in Fig. 3 and Fig. 5, also show sharp peaks, but this is not surprising in the case of the former.

The effect of nuclear transparency does show up at the higher energies where appreciable yields of all three of these reactions are found. This can be explained by the mechanism discussed by Serber<sup>6</sup> in which energies much smaller than the total energy of the incident projectile are obtained from it and utilized by the struck nucleus. This mechanism apparently becomes important at energies sufficiently high so that the collision time between the incident particle and a nucleon in the nucleus is short compared to the time between collisions of the nucleons in the nucleus. The first step in such a high energy nuclear reaction probably involves a collision between the incident particle and an individual nucleon, and the amount of energy transferred to the nucleus depends on the number of subsequent collisions of this type and the

further collisions of the struck nucleons with other particles in the nucleus. This leads to a wide distribution of excitation energies of the struck nucleus. As a consequence an appreciable fraction of struck nuclei are excited to a given energy, say 50 to 75 Mev, even when the incident particles vary in energy from some 100 to 350 Mev, thus supplying the nucleus with the optimum energy and accounting for the continuing high yields of reactions like the (p,6n) and (d,7n). The fact that the relative yield of the reaction at high energies compared to the peak yield with deuterons somewhat exceeds the same ratio for the reaction with protons is probably connected with the fact that the high energy deuteron has its energy divided between its two nucleons and is therefore better suited for the transfer of small amounts of energy to the struck nucleus than is the proton.

It may be of some interest to make a more quantitative comparison between the observed peaks of the excitation curves for the (p,6n) and (d,7n) reactions and what would be predicted on the basis of the compound nucleus idea.

When the excitation of the nucleus is as large as 50 Mev or more, the number of possible competing processes is quite large. For some of the competing processes such as those involving emission of charged particles, one can estimate the corresponding probabilities in a rough way. With 60-Mev excitation, for example, the nuclear temperature of a heavy nucleus like thorium is perhaps about 3 Mev, the Coulomb barrier  $E_c$  for emission of a proton is about 15 Mev. This means that the emission of a proton is at a disadvantage with respect to the emission of a neutron by a factor of the order of  $e^{-E_c/T} = e^{-5} \approx 1/150$ . We have therefore neglected competition from proton emission entirely, and for stronger reasons that from deuteron or alpha-particle emission. A big unknown in the problem, however, is competition from fission. We know for certain that this competition is important. Indirect evidence on this is also obtained from

the relatively low value of the peak cross section for the  $(p,6n)$  and  $(d,7n)$  reaction; it is clear that at the energy corresponding to the peak a large fraction of the total cross section is devoted to fission. The over-all importance of fission is no doubt increased by the fact that fission has a chance to compete with the  $(p,xn)$  and  $(d,xn)$  processes at each successive evaporation of a neutron. Thus a possible, though arbitrary, interpretation of the results is obtained on the assumption of a constant ratio  $\underline{r}$  between neutron width and fission width. The measured ratio of 5 between the heights of the  $\text{Th}(p,3n)$  and  $\text{Th}(p,6n)$  peaks, or what is about the same, between the areas under the two peaks, gives for  $\underline{r}$  the value  $1/(5^{-1/3} - 1)$  which is close to unity, a result strikingly similar to those obtained from experiments at lower excitation energies.

If the ratio  $\underline{r}$  is constant, it is clear that the existence of fission will affect the absolute cross section, but not the shape of the excitation function for a  $(p,xn)$  or  $(d,xn)$  process. The crude calculations described below are made, therefore, neglecting fission altogether.

Other interpretations are no doubt possible. One may assume, for example, that the probability of emission of a neutron increases much more rapidly, with increasing excitation energy, than fission probability. In this case fission competes with neutron emission only in the last stages of the evaporation process, and the number of times such effective competition takes place is independent of the number of evaporations. In this case the lower yield of the  $(p,6n)$  process, with respect to the  $(p,3n)$  process would be attributed to the increased fissionability of the nuclei present during the last stages of the evaporation process; this increased fissionability is expected owing to the decrease in the number of neutrons (increase of the  $Z/A^{1/2}$  ratio).

We do not think that the shape of the excitation curve for, say, a  $(p,6n)$  process will depend in critical manner on the assumed dependence of the fission probability on energy. In view of the present uncertainty about that dependence, it would not be worth while to explore in detail the various possibilities.

In the above-mentioned simple case, in which one may simply forget fission, the problem is fairly simple. We may assume that the probability distribution for the kinetic energy  $\epsilon_n$  of the  $n$ -th neutron is given approximately by a Maxwellian law:  $\epsilon e^{-\epsilon/T} d\epsilon$ , with a temperature  $T$  determined by the residual excitation of the nucleus after  $n-1$  neutrons are emitted. For a heavy nucleus we assume  $T \approx 0.1E^{2/3}$ , where  $E$  is the excitation energy ( $T$  and  $E$  both in Mev). The average value and mean square deviation of  $\epsilon$  are then:

$$\langle \epsilon \rangle = 2T; \quad \langle (\epsilon - \langle \epsilon \rangle)^2 \rangle = 2T^2 \quad (1)$$

For large values of  $\epsilon$  the Maxwellian law fails, and a far better approximation is given by Weisskopf's formula  $\epsilon e^{S(E')/k} d\epsilon$ ,  $S(E')$  being the entropy of the nucleus after the evaporation. Here  $E'$  is the excitation energy after the neutron is emitted,  $E' = E - B - \epsilon$ , if  $B$  is the binding energy of the neutron which for simplicity we regard as independent of  $n$ . It is easy to see that this modification can be approximately taken into account by using for the temperature  $T$  in Equation (1) the temperature evaluated for an excitation  $E - B$ , i.e.,  $T \approx 0.4 (E - B)^{2/3}$ , i.e., roughly speaking the temperature after the evaporation rather than before.

Our problem is, of course, to find the probability of emission of  $x$ , and no more than  $x$  neutrons. This is given by  $P(x) - P(x+1)$ , where  $P(x)$  is the probability of emission of at least  $x$  neutrons, or, in other words, the probability that the first  $x-1$  neutrons are emitted with energies  $\epsilon_1, \dots, \epsilon_{x-1}$  satisfying the condition:

$$E_0 - (x-1)B - \epsilon_1 - \dots - \epsilon_{x-1} > B \quad (2)$$

where  $E_0$  is the initial excitation energy. This is the condition that there be enough energy left for the evaporation of at least another neutron. Knowing the probability distribution of  $\epsilon_1, \epsilon_2, \dots$ , we can estimate the probability that (2) is satisfied. If  $\eta = \epsilon_1 + \epsilon_2 + \dots + \epsilon_{x-1}$ , and  $f(\eta) d\eta$  is the distribution law for  $\eta$  we have:

$$P(x) = \int_0^{E_0 - xB} f(\eta) d\eta \quad (3)$$

So we must first find  $f(\eta)$ . This is given by a very complicated integral, but we know from general theorems that if  $x$  is fairly large one can use "asymptotic" laws, such as the Gauss or the Poisson distribution law. Both laws involve only two arbitrary parameters, which can be expressed in terms of the average value:

$$\langle \eta \rangle = \langle \epsilon_1 \rangle + \dots + \langle \epsilon_{x-1} \rangle \quad (4)$$

and the mean square deviation

$$\sigma^2 = \langle (\eta - \langle \eta \rangle)^2 \rangle = \sum_{n=1}^{x-1} \langle (\epsilon_n - \langle \epsilon_n \rangle)^2 \rangle + 2 \sum_{n=1}^{x-1} \sum_{m=1}^{n-1} \langle (\epsilon_n - \langle \epsilon_n \rangle)(\epsilon_m - \langle \epsilon_m \rangle) \rangle \quad (5)$$

When the root-mean-square deviation  $\sigma$  is small compared to  $\langle \eta \rangle$  the difference between the Gauss and the Poisson law is negligible, but the latter, i.e.:

$$f(\eta) d\eta = \left[ s^s / \Gamma(s) \right] (\eta / \langle \eta \rangle)^{s-1} e^{-s\eta / \langle \eta \rangle} d\eta / \langle \eta \rangle \quad (6)$$

$$s = \langle \eta \rangle^2 / \sigma^2 \quad (7)$$

is preferable since Gauss' law extends to negative values of  $\eta$ , which are physically meaningless. Once the average values (4) and (5) are known, the exponent  $s$  is given by (7) and we can evaluate the integral (3) by means of

a Table of the incomplete gamma function.

The main remaining difficulty is that the variables  $\epsilon_1, \epsilon_2, \dots$  are statistically dependent, since the temperature for  $\epsilon_2$  depends on  $\epsilon_1$ , the temperature for  $\epsilon_3$  depends on  $\epsilon_1 + \epsilon_2$ , etc.... The difficulty, however, can be circumvented by a recurrent procedure, in which use is made of the fact that the temperature  $T$  is a slowly variable function of the excitation energy. Thus if

$$\zeta = \epsilon_1 + \epsilon_2 + \dots + \epsilon_x = \eta + \epsilon_x$$

we have

$$\langle \zeta \rangle = \langle \eta \rangle + \langle \epsilon_x \rangle = \langle \eta \rangle + 2 \langle T \rangle$$

where  $T$  is now the temperature for the emission of the  $x$ -th neutron, or according to our previous discussions:

$$T = T(\eta) = 0.4(E_0 - xB - \eta)^{1/2} \quad (8)$$

As a first approximation we may set  $\eta = \langle \eta \rangle$  in (8) and obtain a  $T(\langle \eta \rangle) = T_1$  say. Then expanding (8) in powers of the difference  $\eta - \langle \eta \rangle$ :

$$T(\eta) = T(\langle \eta \rangle) + (dT/d\eta)(\eta - \langle \eta \rangle) + 1/2(d^2T/d\eta^2)(\eta - \langle \eta \rangle)^2 + \dots \quad (9)$$

Now to obtain  $\langle \epsilon_x \rangle$  according to Equation (1) we must take twice the average of (9). In this manner we obtain finally:

$$\langle \zeta \rangle = \langle \eta \rangle + 2T(\langle \eta \rangle) \left\{ 1 - \langle (\eta - \langle \eta \rangle)^2 \rangle / (E_0 - xB - \langle \eta \rangle)^2 \right\} \quad (10)$$

In a similar manner we compute:

$$\langle (\zeta - \langle \zeta \rangle)^2 \rangle = \langle (\eta - \langle \eta \rangle)^2 \rangle + \langle (\epsilon_x - \langle \epsilon_x \rangle)^2 \rangle + 2 \langle (\eta - \langle \eta \rangle)(\epsilon_x - \langle \epsilon_x \rangle) \rangle \quad (11)$$

For instance in the last term, we again use the fact that  $\langle \epsilon_x \rangle$  is  $2T(\eta)$  averaged over  $\eta$  and write  $\epsilon_x - \langle \epsilon_x \rangle = \epsilon_x - 2T(\eta) + 2T(\eta) - \langle \epsilon_x \rangle$  (12)

Then:

$$\langle (\eta - \langle \eta \rangle)(\epsilon_x - \langle \epsilon_x \rangle) \rangle = \langle (\eta - \langle \eta \rangle)(\epsilon_x - 2T(\eta)) \rangle + \langle (\eta - \langle \eta \rangle)(2T(\eta) - \langle \epsilon_x \rangle) \rangle \quad (13)$$

The averaging can be done first over  $\epsilon_x$  for a given  $\eta$ , then over  $\eta$ . The first term on the right of Equation (13) is zero, the second is evaluated expanding  $T(\eta)$  as before. Finally one gets:

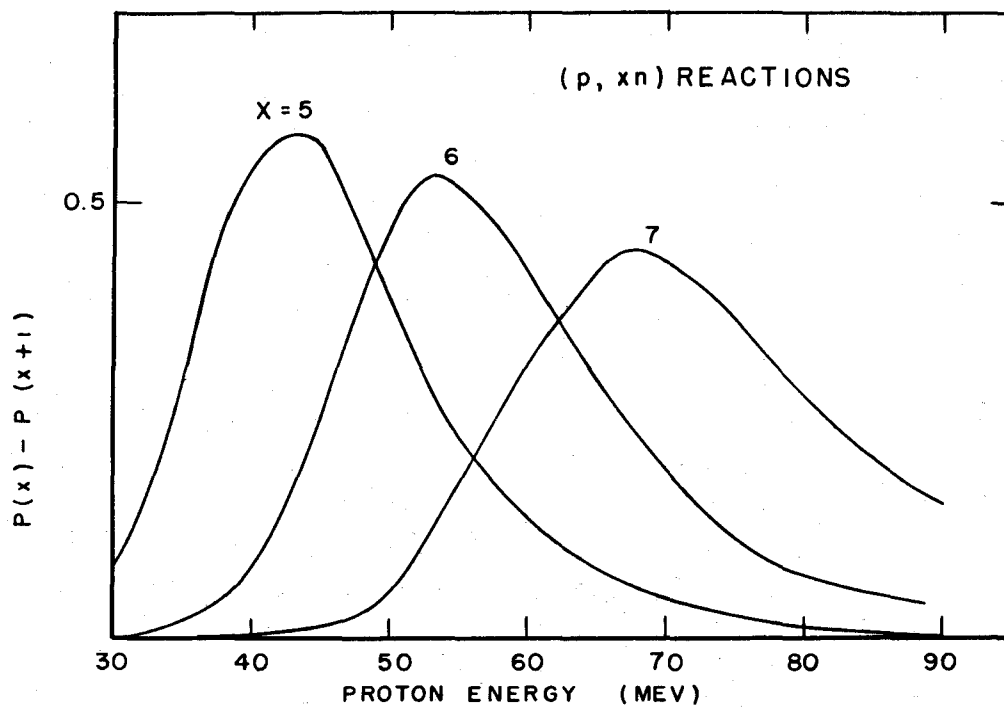
$$\begin{aligned} \langle (\xi - \langle \xi \rangle)^2 \rangle &= \langle (\eta - \langle \eta \rangle)^2 \rangle + 2T^2(\langle \eta \rangle) - \langle (\eta - \langle \eta \rangle)^2 \rangle \left\{ 2T(\langle \eta \rangle)(E_0 - xB - \langle \eta \rangle)^{-1} - \right. \\ &\quad \left. T^2(\langle \eta \rangle)(E_0 - xB - \langle \eta \rangle)^{-2} \right\} \end{aligned} \quad (14)$$

Equations (10) and (14) allow one to compute the average and standard deviation of  $\xi$  (which is  $\eta$  for  $x+1$  neutrons) in terms of the same quantities for  $\eta$ .

This recurrent scheme has been carried out for several values of the excitation energy  $E_0$ . Then the probability of emission of  $x$  and only  $x$  neutrons was obtained in the manner indicated above. The curves obtained, Fig. 10, show a striking similarity with the  $(p,6n)$  results. There is a slight displacement of the experimental maximum towards higher energies (remember also that the excitation energy is the kinetic energy) which is not very significant in view of the fact that the range-energy relation has not been gauged accurately. In fact, the lower value of the threshold obtained in the case of the  $(d,7n)$  reaction, where a more accurate comparison was done may well indicate a small systematic error in the desired direction in the proton case. Otherwise the general appearance and in particular the width of the curves are in fair agreement.



Fig. 10. Probability of emission of  $x$  neutrons after capture of a proton. For deuterons decrease the energy values by 4 Mev.



MU 846

Fig. 10

The excitation functions for the  $(\alpha, p8n)$  and  $(\alpha, p5n)$  reactions shown in Figs. 8 and 9 have very broad maxima as distinguished from the indicated sharp peaks and lower yields for the  $(\alpha, 6n)$  and  $(\alpha, 7n)$  excitation functions (the data for which were discussed in Section II-C-3). There are two factors which contribute to this difference between the two types of reactions. First, in the  $(\alpha, pxn)$  reaction the potential barrier for the proton makes it necessary for the proton to carry with it more energy than an emitted neutron and therefore makes it possible to utilize extra energy to advantage. The second factor is connected with the complex nature of the helium ion, consisting of four nucleons with a possible uneven division of the kinetic energy between them at the time of impact. In the case of the  $(\alpha, pxn)$  reaction, only one proton from the helium ion need be retained by the struck nucleus. The  $(\alpha, xn)$  reaction demands a retention of two protons and hence a much closer approach to the formation of a compound nucleus.

The faster fall off in yield with increasing energy of the  $(\alpha, p5n)$  compared to the  $(\alpha, p8n)$  reaction is reasonable in view of the smaller energy requirement of the former. It is interesting to note that the excitation function for the  $(p, \alpha 8n)$  reaction shown in Fig. 4 presents a broad peak at a position toward the full energy of the incident proton. This is undoubtedly connected with the potential barrier for the outgoing alpha-particle (or two protons), which can use relatively large amounts of energy to advantage.

It is unfortunate that the spread in energy of the bombarding particles is so great as to make it impossible to determine accurate threshold values for the various reactions. The rough result of about 40 Mev which was obtained for the  $(d,7n)$  reaction by comparison with reactions of known threshold determined with precision with low energy particle accelerators as shown in Fig. 7 indicates an average binding energy of about 7 to 7.5 Mev per neutron. This is a very reasonable value and can probably be used to estimate thresholds for  $(d,xn)$  and  $(p,xn)$  reactions in this region.

The excitation functions which have been determined in this work serve the very practical purpose of making it possible to estimate the optimum energy for the production of the maximum specific activity for isotopes produced by these and similar reactions. The results also suggest that in the case of  $(p,xn)$  and  $(d,xn)$  reactions, perhaps even when  $x$  is as large as 10, the peaks are sufficiently sharp to make it possible to make isotopic assignments of new activities by measuring their excitation functions.

## V. EXPERIMENTAL DETAILS

### A. 184-inch Cyclotron Beam Types

With the Berkeley 184-inch cyclotron, there are three ways the charged particle beam can be used: as an internal beam, as an external beam, and as an electrostatically deflected beam. For use in the internal beam a target can be inserted on a probe into the tank of the cyclotron to intercept the beam at

any desired radius from about 20 inches up to the full radius of 81 inches. At present it is possible to obtain an internal beam current of about one microampere of deuterons or protons, and about 0.1 microampere of helium ions.

When the beam is brought out of the vacuum tank through thin aluminum windows and led into an external "cave," the external beam so produced has several advantages. Its energy definition is good (one-half to one percent spread); it can be collimated to any desired shape and is very adaptable to experiments; it can be made to intercept the center of a target foil; and it does not require that the target be in a vacuum, thus greatly increasing the number of bombardment possibilities. These advantages are obtained at the expense of a great sacrifice in beam current which for the proton or deuteron beam is reduced to  $10^{-5}$  to  $10^{-4}$  microamperes. This, except in rare cases, is not enough to be very useful for chemical investigations of reactions with cross sections of  $10^{-2}$  barns or less.

Many of the advantages of the external beam are secured with a much less severe beam reduction by use of the electrostatically deflected beam.<sup>14</sup> This beam is produced by applying a pulsed voltage to a deflector electrode as the internal beam pulse reaches its maximum orbit of 81 inches. The particles are pushed in from their maximum orbit and when they pass the end of the  $120^\circ$  arc of the deflector, they again move in an orbit of radius close to 81 inches but with center displaced so that the beam now intercepts the middle of a target at a distance from the center of about 83 inches. The particles can be maximized on a certain portion of the target by adjusting the amount of voltage applied to the deflector. The reduction in intensity from that of the internal beam is a factor of 50 or more but in most of the reactions here studied, this could be tolerated.

---

<sup>14</sup>Powell, Henrich, Kerns, Sewell, and Thornton, Rev. Sci. Instruments 19, 506 (1948).

### B. Methods of Varying the Beam Energy; Calculations and Errors Involved

A straightforward method of running excitation function bombardments is to place the target probe at different radial positions in the full undeflected internal beam in successive bombardments. No absorbers are required and the beam energy is closely defined by the radius. The only energy spread is that of the incident beam since no further energy spread or straggling is introduced by passage through a thick absorber stack. When the cross section of the nuclear reaction being studied is low and/or the half-life or radiation characteristics of the product nucleus make it necessary to maximize the absolute yield of the product, the use of this method is clearly indicated. The principal objection lies in the difficulty of duplicating precisely the beam current and beam position in successive bombardments. To correct for these fluctuations, it is necessary to bombard with each target foil a monitor foil which undergoes some nuclear reaction for which an excitation function has previously been determined. Examples of useful monitor reactions are  $C^{12}(d,n)N^{13}$ ,  $Al^{27}(d,ap)Na^{24}$  and  $Al^{27}(p,3pn)Na^{24}$ . Polystyrene foils are commonly employed for the first reaction.

The stacked foil technique has been used most frequently (see Appendix). Weighed target foils either alone or separated by intermediate absorber foils of aluminum or copper can be used to reduce the beam energy. A variation of this method is the bombardment of a thick target followed by the successive milling off of thin layers and the determination of the yield in each layer. This method in either variation is best performed with the deflected beam.

The range-energy relationships calculated by the Theoretical Physics Group at the University of California Radiation Laboratory were used in the present work to convert from absorber thickness to energy of the transmitted particles.<sup>8</sup> These data have been published in graphical form.<sup>7</sup>

The following values were taken for the maximum particle energies and the corresponding ranges in copper: 348-Mev protons,  $97,250 \text{ mg/cm}^2$ ; 194-Mev deuterons,  $22,420 \text{ mg/cm}^2$ ; and 388-Mev helium ions,  $11,260 \text{ mg/cm}^2$ . The total amount of absorber up to the middle of each foil was converted, for convenience, to equivalent thickness ( $\text{mg/cm}^2$ ) of copper and after subtraction from the full range value the difference was used to determine the energy from the proper range-energy relationship.

In this work the materials in the beam included copper, thorium, uranium, aluminum, and polystyrene foils. Range-energy relationships<sup>7</sup> were available for all three particles in copper and aluminum and for protons in carbon (from which that for deuterons in carbon could be calculated). It is assumed that carbon atoms alone are responsible for the stopping power of the polystyrene. In order to obtain values for thorium and uranium the values given for lead were extrapolated by means of the relationship,  $Z/A \times \text{Range} = \text{Constant}$ . This extrapolation is sufficiently accurate for the present purpose since the change in range is only about two percent between lead and thorium in terms of weight per unit area. Most of the beam energy reduction occurred in the copper and the relatively smaller amounts of thorium or uranium were converted to copper equivalents by the following method. The copper equivalent, for example, of a certain amount of thorium was determined by calculating the ratio of the difference in range in thorium between the two energy values to that for copper and dividing the amount of thorium ( $\text{mg/cm}^2$ ) by this figure.

There are two major uncertainties involved in the use of the stacked foil technique which tend to spread out a peak in an excitation function experiment, particularly if the peak occurs at relatively low energies. First, there is the initial energy distribution of the beam. There is apparently an energy spread of up to three percent in the 184-inch cyclotron full energy internal

beam and electrostatically deflected beam, and of about one percent in the external beam. When protons of initial maximum energy 348 Mev are reduced to 50 Mev by copper absorbers, an initial spread of one percent in energy corresponds to a spread of about 15 Mev, and an initial three percent spread corresponds to about 50 Mev, at the 50-Mev level.

The other effect which contributes to the spreading out of the excitation function peaks so as to give falsely large widths, is the straggling of the particle beams. Calculation of the extent of this is possible; a calculation indicating the straggling of 348-Mev protons introduced by passage through copper has been made by W. Aron of the Theoretical Physics Group of the Radiation Laboratory. From his calculations it is seen that at 100 Mev, the energy "width" due to straggling is about 4.3 Mev, while at 50 Mev it has increased to about 7.3 Mev. These figures represent root-mean square deviations. In order to compare them with the above figures for the initial energy distribution let us assume, for instance, that we have to do with a square distribution law, i.e., constant intensity within an interval of three percent width, and zero outside. The standard deviation in energy corresponding to this is  $3 \cdot 12^{-1/2}$  percent or 0.87 percent. When protons of initial maximum energy 348 Mev are reduced to 50 Mev by copper absorbers, an initial deviation of 0.87 percent in energy corresponds to a final root-mean square deviation in energy of 11.1 Mev which is slightly larger than the effect of straggling at the 50-Mev level. It must be remembered, of course, that the initial energy spread of the beam can vary with the setting of the deflector, so that data obtained from one experiment cannot be applied directly to another experiment, even though conditions were very much the same.



These two effects lead to peaks which are appreciably wider than their true widths as illustrated by comparison of the results shown in Fig. 7 with those given for the same reactions as determined with machines which give low energy particles directly.<sup>12,13</sup> Another striking example of this comes from the work of E. L. Kelly who used the value of 388 Mev for the most probable maximum energy of the helium ion beam and roughly matched the peak energy on a  $\text{Bi}^{209}(\alpha, 2n)\text{At}^{211}$  excitation curve taken through the use of aluminum absorbers with the electrostatically deflected beam of the 184-inch cyclotron<sup>3</sup> with a curve for the same reaction taken very carefully with the 39 Mev external helium ion beam of the 60-inch Berkeley cyclotron.<sup>15</sup> In these experiments the width of the peak at half maximum for the electrostatically deflected beam determination was about 500 mg/cm<sup>2</sup> of aluminum compared to about 116 mg/cm<sup>2</sup> of aluminum on the 60-inch cyclotron.

It is clear that, since the effect of straggling can be estimated theoretically, and the relevant formulae are considered reliable, comparisons like those just made can be used to estimate, in a manner independent from other information, the energy spread of the initial beam. A very good example is the  $\text{C}(d, n)$  reaction of Fig. 7. The excitation curve from low energy machines plotted on a range scale would consist of a sharp peak of negligible width. The effect of straggling transforms this into a gaussian peak with a standard deviation of 150 mg/cm<sup>2</sup> of Al (this is the range straggling for reduction of a deuteron from 190 Mev to practically zero energy). The actually observed peak has a standard deviation about 3/2 of that obtained from straggling alone. Thus the effects of straggling and initial energy distribution are comparable in good agreement with the previous estimate.

---

<sup>15</sup>E. L. Kelly and E. Segrè, Phys. Rev. 75, 999 (1949).

Since the 348-Mev protons generated by the 184-inch cyclotron have a range of about 4.3 inches of copper, thick copper absorbers were required to decrease the beam energy between the thorium target foils. Because of this long range, an appreciable fraction of the beam in its progress through the stack is absorbed by producing nuclear reactions in the copper so that the beam is not only degraded in energy but is also attenuated. Rough correction factors for this effect were obtained from measurements made by V. Peterson of the Radiation Laboratory who measured the amount of absorption of the proton beam in copper blocks of known thickness. A plot of the data, absorber thickness vs. transmission, shows an exponential dependence for the experimental arrangement used, with a transmission of about 0.6 for 70 g/cm<sup>2</sup> copper absorber, the data being good to about 20 percent. A correction for this nuclear absorption has been applied to the yield calculations for all of the samples from proton bombardments. No corrections were made in the case of the deuteron and helium bombardments, where the ranges are so much less as to make the error introduced smaller.

### C. Experimental Details in Use of the Three Beam Types

1. Internal Beam Bombardments.-- The small amount of U<sup>230</sup> and U<sup>229</sup> alpha-activity produced by the Th<sup>232</sup>( $\alpha$ ,6n) and Th<sup>232</sup>( $\alpha$ ,7n) reactions made it necessary to use the internal beam for the determination of their excitation functions. Thin foils were mounted on the probe and the beam energy determined by an accurate determination of the radius to the leading edge of the foil. The target thickness in each case was only a few percent of the total range of the incident particles.

Attempts were made to use the stacked foil technique in the internal beam, but the runs were unsatisfactory since the variation of the angle of incidence of the internal beam served to spread out and falsify the peaks of the excitation functions studied.

2. External Beam Measurements.--- The reaction cross sections and product isotope decay characteristics were not favorable enough in the reactions studied here to permit use of the external beam except for absolute yield determinations in the two most favorable cases. These two were the reactions  $\text{Th}^{232}(\text{p}, 6\text{n})\text{Pa}^{227}$  and  $\text{Th}^{232}(\text{d}, 7\text{n})\text{Pa}^{227}$ . Even here only a few thousand disintegrations of  $\text{Pa}^{227}$  per minute at shutdown were obtained from 40-min. bombardments of 5-mil thorium at full energy. In these experiments the current passing through the target was collected and measured in a Faraday cup.

3. Electrostatically Deflected Beam Experiments.--- Most of the experiments were run in the electrostatically deflected beam with the use of the apparatus shown in Fig. 10. In this apparatus accurately weighed copper absorbers of various thicknesses with sides milled parallel to within 0.2 mils were employed to reduce the beam energy. As much as 4.3 inches of copper could be inserted to ensure complete stoppage of the most energetic beam (348-Mev protons). The 5-mil target material in the form of 3/4 inch diameter metal discs was fastened by small pieces of scotch tape (1/4 inch to 1/8 inch) to masks of 5-mil copper and thus located 3/4 of an inch from the beam side edge and midway between top and bottom of the copper absorbers. The copper on the beam side of the target material serves the very important function of reducing the background due to particles coming in from the side of the absorber stack to about one-hundredth (or less in some cases) of the maximum activity of the excitation curve. A support ledge is provided on the beam side of the absorber stack to permit the addition of more absorber if it should become necessary

Fig. 11. Excitation function apparatus.



to reduce this background further.

The 1-1/2 inch thick copper collimator with the 3/4 inch collimating hole was used in front of the absorber stack to increase the definition in the deuteron and helium ion bombardments. It was possible to obtain reproducibly good results without it as shown by the proton bombardments in which it could not be used for lack of space. The use of the collimator where possible actually increased the yields of activity by a factor of 20 or more; this results from the fact that the collimator, being grounded, allows the beam current to be maximized on the target foils themselves, rather than to strike haphazardly on the block of absorbers, which ensures that the target foils are hit by the "hot spot" of the beam.

Other details of the apparatus are designed to ensure the absorbers in the stack being held rigidly in place.

When the apparatus is assembled, the copper current-reading contact rests upon the absorber stack which is insulated from the rest of the apparatus both by the "Dilectine" insulator tray and by pieces of mica between the stack and the absorber shield which is grounded to the absorber support. It is necessary to shield the absorber stack electrically from the external electrostatic fields which would influence the current readings and the copper box is used for this purpose. This absorber shield is kept in position by two screws on each end of the absorber support. The beam passes through a thin copper foil window in the shield, this window thickness being included in the range energy calculations. The entire apparatus fits onto the standard cyclotron probe head.

Immediately after bombardment the four centering screws are loosened, the absorber shield removed with a pair of tongs by a small hook which is not shown on the drawing, the bolt on the absorber stack loosened, a small rod slipped through the tab holes in the masks, and the masks lifted free. The

target discs are removed from the masks in the chemical laboratory and subjected to the chemical operations described below.

To maximize the beam on the target, it is possible to vary both the radius of the target apparatus and the voltage on the deflector. Furthermore, the entire tray of absorbers can be raised or lowered to position the targets vertically in the beam by loosening the wing nuts holding the absorber support as shown in the insert in the drawing.

With this apparatus and suitable absorbers, it is possible to determine simultaneously as many as 16 points on an excitation curve (with a minimum interval of 5 Mev between points for alpha bombardments and much less for deuteron and proton bombardments).

#### D. Chemical Procedures for Protactinium and Uranium Separation

The only essential requirement of the chemical procedure is that the amount of interfering radioactivity be reduced quickly to such a degree that the product isotopes of interest can be accurately measured through some characteristic radiation (in the present case by the alpha-particles of characteristic energy and half-life). However, these are severe requirements when it is considered that (1) an exceedingly complex mixture of radioactivities is produced (2) up to 16 samples must be processed and counted before the short-lived activities (such as the 38.3-min.  $\text{Pa}^{227}$ ) have disappeared (3) the chemical yields must be reproducible (4) the final samples must be virtually weightless to permit accurate determination of the alpha-particle energy spectrum.

The following separation procedure based on the solvent extraction of an organic complex ion of the element fulfilled the above conditions for protactinium. Studier, Hagemann, Hyde<sup>16</sup> and others were the first to apply to bombardment

---

<sup>16</sup>Studier, Hagemann, Jr., and Hyde, unpublished work (1945).

chemistry the fact that protactinium forms a complex with the  $\beta$ -diketone thenoyl-trifluoroacetone<sup>9</sup> (TTA) which is soluble in benzene and other organic solvents and may be extracted from a strongly acidic aqueous solution. Many other elements form solvent extractable TTA complexes but no other alpha-particle emitting element except protactinium will extract from strongly acidic solution.

In the chemical procedure<sup>17</sup> each thorium (~0.4 gram) or uranium (~0.7 gram) disc was dissolved in a 125 ml Phillips beaker with 10 ml concentrated nitric acid and, in the case of thorium, one drop of 0.2M ammonium fluosilicate solution. The solution was heated gently on a hot plate until the reaction started. The solution was diluted with 10 ml of water and transferred into a separatory funnel (consisting of a 40 ml calibrated centrifuge cone with a stopcock sealed to the bottom). The mass production arrangement is shown in Fig. 11. Ten ml of 0.4M thenoyltrifluoroacetone (TTA) in benzene solution was added and the mixture stirred for five minutes. The aqueous and organic layers for each sample were collected in separate tubes and about half of the organic layer (containing the protactinium) evaporated on a platinum disc, ignited to destroy the organic matter and form a weightless film, and counted for gross alpha-disintegration rate. The evaporations were made carefully to prevent loss of protactinium which was especially necessary in the case of the uranium bombardments. Fig. 12 shows the apparatus for the simultaneous evaporation of 16 samples. The 1/4 inch washers shown were used to raise the platinum discs above the surface of the hot plate and thus allow loading of as much as 1 ml of the benzene solution at a time. It has been possible to start counting the samples from a run of 16 foils as early as 110 minutes after the end of bombardment. This protactinium

---

<sup>17</sup>W. W. Meinke, U. S. Atomic Energy Commission Declassified Documents  
AECD-2738 (Aug., 1949) and AECD-2750 (July-Aug., 1949).



Fig. 12. Apparatus for simultaneous extraction of  
16 samples into TTA-benzene solution.

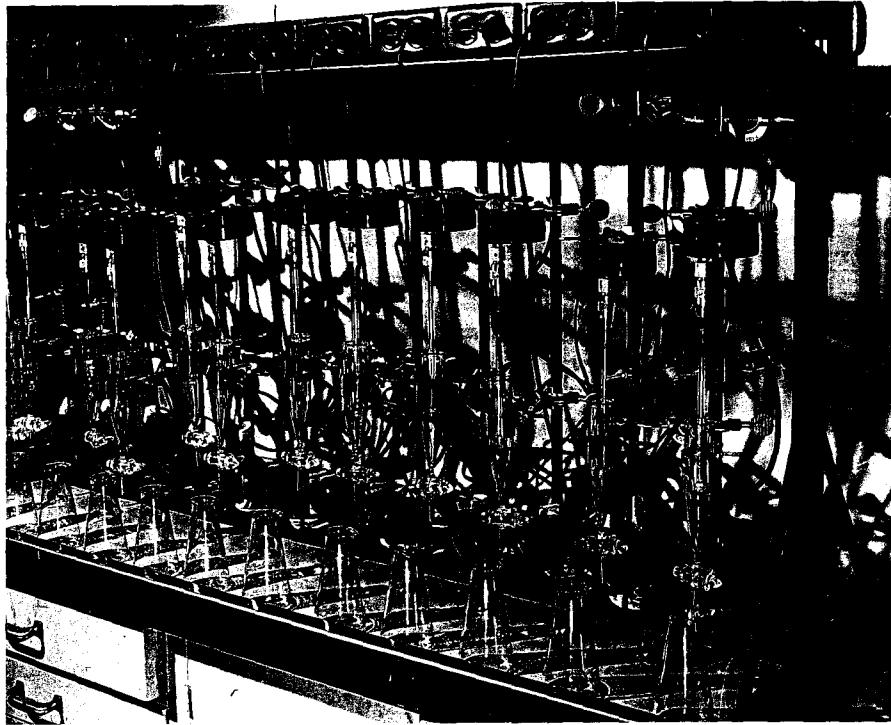


FIGURE 12

Fig. 13. Set-up for simultaneous evaporation of sixteen 10-ml samples on platinum plates.



FIGURE 13

procedure worked smoothly when applied to thorium targets, somewhat erratically but still for the most part consistently when applied to uranium targets.

The chemical yields of the runs reported in this paper are consistent among themselves to within five to ten percent, but the absolute chemical yield has in most cases been left undetermined. It is known that the majority of the protactinium is extracted in the one equilibration with TTA-benzene solution.

The absolute cross sections for the reactions  $\text{Th}^{232}(\text{p},6\text{n})\text{Pa}^{227}$  and  $\text{Th}^{232}(\text{p},7\text{n})\text{Pa}^{227}$  were determined for runs made with the external beam as mentioned previously. In these runs the chemical yield of protactinium was determined with the use of  $\text{Pa}^{231}$  tracer. Precautions were taken to eliminate the uncertainties frequently encountered in the exchange of  $\text{Pa}^{231}$  tracer because of unknown ionic or colloidal species formed on standing in aqueous solutions particularly of low acidity, but it is not certain that this was accomplished successfully. Therefore, the absolute yields reported are subject to some question.

The efforts to develop a uranium purification procedure for the  $\text{Th}(\alpha,\text{xn})\text{U}$  studies were not very satisfactory. An ether extraction procedure of the type described by Newton<sup>18</sup> suggested itself as a very promising starting point, but in attempting to reduce this to a minimum-step procedure suitable for the simultaneous processing of 16 samples with enough speed to detect a one-hour half-life, difficulties developed. Some success in removing all extraneous activities from a uranium fraction was attained with a more lengthy procedure similar to that devised by Crane.<sup>17</sup> It involves precipitation of the uranium on lanthanum hydroxide, followed by dissolution and removal of impurities by zirconium iodate precipitations from the uranyl solution, in addition to the ether extractions. The yield has been found to be rather low (less than ten percent), unless extra time is spent in increasing it by re-extractions and re-precipitations.

---

<sup>18</sup>A. S. Newton, Phys. Rev. 75, 209 (1949).

### E. Counting and Pulse Analysis Measurements

The alpha-particle emission rate of the samples was determined in an ordinary argon ionization chamber in which 50-52 percent of the particles are detected. A standard scale of 512 scaling circuit was used and the measured counting rates were such that coincidence corrections were not necessary. The decay of the emission rate was followed to identify the half-life in question. Appropriate allowance was made for the contribution of daughters to the gross activities in calculating the true counting rate of the parent itself.

In many cases it was necessary to subject the samples to alpha pulse analysis with the 48-channel differential pulse analyzer.<sup>10</sup> Pulse analysis was especially important in determining the amount of beta-particle emitting  $\text{Pa}^{230}$  by measurement of the amount of the alpha-emitting  $\text{U}^{230}$  daughter present several weeks after bombardment. The amount of  $\text{Pa}^{230}$  initially present was calculated by means of the appropriate daughter growth equation and decay constants,<sup>19</sup> allowing for the ten percent branching decay of  $\text{Pa}^{230}$  by negative beta-particle emission reported by Studier and Bruehlman.<sup>11</sup>

In the experiments in which the beta-particle emission rate of the polystyrene and aluminum targets were measured, an end-window, bell-type Geiger tube filled with a 9 cm argon and 1 cm ethyl alcohol gas mixture was employed. The thickness of the mica window was 3 mg/cm<sup>2</sup>. Samples were placed 7.0 cm below the counter window, where a geometrical counting yield of 1.7 percent obtains. A scale of 64 scaling circuit was used and a coincidence correction of 1.2 percent per thousand pulses per minute was applied to all counting rates.

All of the alpha-disintegration rates plotted in the graphs have been corrected for decay back to the end of bombardment and refer to the isotope in

---

<sup>19</sup> M. H. Studier and E. K. Hyde, Phys. Rev. 74, 591 (1948).

question (i.e., the gross counting rates have been corrected for activity due to the daughter isotopes). The relative yields were normalized to 0.4 gram thorium, 0.7 gram uranium, 0.1 gram aluminum, or 0.04 gram polystyrene. In those cases where more than one run on a certain reaction was made, the one that was considered most accurate or more consistent was taken as a standard and the yields of the other runs normalized to it. In one of the runs on the  $\text{Th}^{232}(\text{d},7\text{n})$  reaction a mistake was apparently made in tabulating the absorbers, in which one absorber was overlooked, and the results without correction gave a plot with the peak shifted about 12 Mev. In this case the error in tabulation was assumed and the corresponding correction was made in plotting the data in Fig. 5.

## VI. ACKNOWLEDGMENT

We wish to thank James T. Vale and the crew of the 184-inch cyclotron for their assistance in carrying out this work. It is a pleasure to acknowledge the interest of Professors E. M. McMillan and I. Perlman, and of Earl K. Hyde and Albert Ghiorso in this problem. We would also like to express our appreciation to Herman P. Robinson for his help in the design and procurement of equipment; and to W. A. Aron, B. G. Hoffman, and F. C. Williams, and to V. Peterson for permission to include material not published elsewhere. This work was carried out under the auspices of the U. S. Atomic Energy Commission.

## APPENDIX

### Bibliography of Thin Target Excitation Functions For Charged Particle Reactions

#### A. Deuterons

##### 1.9 Mev:

$\text{Na}^{23}(\text{d},\text{p})\text{Na}^{24}$  - E. O. Lawrence, Phys. Rev. 47, 17 (1935).

$\text{Al}^{27}(\text{d},\text{p})\text{Al}^{28}$  - E.M. McMillan and E. O. Lawrence, Phys. Rev. 47, 343 (1935).

(Historically the first use of the stacked foil technique with accelerated particles.)

##### 2.8 Mev:

$\text{C}^{12}(\text{d},\text{n})\text{N}^{13}$  - C. L. Bailey, M. Phillips, and J. H. Williams, Phys. Rev. 62, 80 (1942).

##### 3.5 Mev:

$\text{Mg}^{26}(\text{d},\text{p})\text{Mg}^{27}$ ;  $\text{Mg}^{26}(\text{d},\alpha)\text{Na}^{24}$  - M. C. Henderson, Phys. Rev. 48, 855 (1935).

$\text{Na}^{23}(\text{d},\text{p})\text{Na}^{24}$ ;  $\text{Al}^{27}(\text{d},\text{p})\text{Al}^{28}$ ;  $\text{Si}^{30}(\text{d},\text{p})\text{Si}^{31}$ ;  $\text{Cu}^{63}(\text{d},\text{p})\text{Cu}^{64}$  - E. O. Lawrence,

E.M. McMillan, and R. L. Thornton, Phys. Rev. 48, 493 (1935).

$\text{C}^{12}(\text{d},\text{n})\text{N}^{13}$ ;  $\text{N}^{14}(\text{d},\text{n})\text{O}^{15}$ ;  $\text{O}^{16}(\text{d},\text{n})\text{F}^{17}$  - H. W. Newson, Phys. Rev. 48, 790 (1935).

##### 5 Mev:

$\text{C}^{12}(\text{d},\text{n})\text{N}^{13}$ ;  $\text{N}^{14}(\text{d},\text{n})\text{O}^{15}$ ;  $\text{O}^{16}(\text{d},\text{n})\text{F}^{17}$  - H. W. Newson, Phys. Rev. 51, 620 (1937).

$\text{A}^{40}(\text{d},\text{p})\text{A}^{41}$  - A. H. Snell, Phys. Rev. 49, 555 (1936).

$\text{Ni}^{60}(\text{d},\text{n})\text{Cu}^{61}$  - R. L. Thornton, Phys. Rev. 51, 893 (1937).

$\text{Cu}^{63}(\text{d},\text{p})\text{Cu}^{64}$  - S. N. Van Voorhis, Phys. Rev. 50, 895 (1936).

##### 6 Mev:

$\text{Pd}^{108}(\text{d},\text{p})\text{Pd}^{109}$ ;  $\text{Pd}^{110}(\text{d},\text{n})\text{Ag}^{111}$  - J. D. Kraus and J. M. Cork, Phys. Rev. 52, 763 (1937).

$\text{Al}^{27}(\text{d},\text{p})\text{Al}^{28}$ ;  $\text{Si}^{30}(\text{d},\text{p})\text{Si}^{31}$  - W. Riezler, Naturwiss. 34, 157 (1947).



9 Mev:

$\text{Fe}^{54}(\text{d},\text{n})\text{Co}^{55}$  - J. M. Cork and B. R. Curtis, Phys. Rev. 55, 1264 (1939).

$\text{Pb}^{206}(\text{d},2\text{n})\text{Bi}^{206}$ ;  $\text{Pb}^{208}(\text{d},\text{p})\text{Pb}^{209}$  - K. Fajans and A. F. Voigt, Phys. Rev. 60, 619 (1941).

$\text{U}^{238}(\text{d},\text{p})\text{U}^{239}$  - N. Feather and R. S. Krishnan, Proc. Camb. Phil. Soc. 43, 267 (1947).

$\text{Th}^{232}(\text{d},\text{fiss})$ ;  $\text{U}^{238}(\text{d},\text{fiss})$  - D. H. T. Gant and R. S. Krishnan, Proc. Roy. Soc. London A178, 474 (1941).

$\text{Bi}^{209}(\text{d},\text{n})\text{Po}^{210}$ ;  $\text{Bi}^{209}(\text{d},\text{p})\text{Bi}^{210}$  - D. G. Hurst, R. Latham, and W. B. Lewis, Proc. Roy. Soc. London A174, 126 (1940).

$\text{Th}^{232}(\text{d},\text{fiss})$ ;  $\text{U}^{238}(\text{d},\text{fiss})$  - I. C. Jacobsen and N. O. Lassen, Phys. Rev. 58, 867 (1940).

$\text{Ag}^{107}(\text{d},\text{p}2\text{n})\text{Ag}^{106}$  - R. S. Krishnan and T. E. Banks, Nature 145, 777 (1940).

$\text{F}^{19}(\text{d},\text{H}^3)\text{F}^{18}$  - R. S. Krishnan, Nature 148, 407 (1941).

$\text{Ag}^{107}(\text{d},\text{p})\text{Ag}^{108}$ ;  $\text{Ag}^{107}(\text{d},\text{H}^3)\text{Ag}^{106}$ ;  $\text{Ag}^{107}(\text{d},2\text{n})\text{Cd}^{107}$ ;  $\text{Ag}^{109}(\text{d},2\text{n})\text{Cd}^{109}$  - R. S. Krishnan, Proc. Camb. Phil. Soc. 36, 500 (1940).

$\text{Au}^{197}(\text{d},\text{p})\text{Au}^{198}$ ;  $\text{Au}^{197}(\text{d},2\text{n})\text{Hg}^{197}$  - R. S. Krishnan, Proc. Camb. Phil. Soc. 37, 186 (1941).

$\text{Cu}^{63}(\text{d},\text{p})\text{Cu}^{64}$ ;  $\text{Cu}^{63}(\text{d},\text{H}^3)\text{Cu}^{62}$ ;  $\text{Sb}^{121}(\text{d},\text{p})\text{Sb}^{122}$ ;  $\text{Sb}^{121}(\text{d},\text{H}^3)\text{Sb}^{120}$  - R. S. Krishnan and T. E. Banks, Proc. Camb. Phil. Soc. 37, 317 (1941).

$\text{Pt}^{196}(\text{d},\text{p})\text{Pt}^{197}$ ;  $\text{Pt}^{198}(\text{d},\text{p})\text{Pt}^{199}$  - R. S. Krishnan and E. A. Nahum, Proc. Camb. Phil. Soc. 37, 422 (1941).

$\text{Au}^{197}(\text{d},\text{p})\text{Au}^{198}$ ;  $\text{Au}^{197}(\text{d},2\text{n})\text{Hg}^{197}$ ;  $\text{Tl}^{205}(\text{d},\text{p})\text{Tl}^{206}$ ;  $\text{Tl}^{205}(\text{d},2\text{n})\text{Pb}^{205}$ ;  $\text{Pb}^{208}(\text{d},\text{p})\text{Pb}^{209}$ ;  $\text{Bi}^{209}(\text{d},\text{p})\text{Bi}^{210}$ ;  $\text{Bi}^{209}(\text{d},\text{n})\text{Po}^{210}$ ;  $\text{Th}^{232}(\text{d},\text{p})\text{Th}^{233}$  -

R. S. Krishnan and E. A. Nahum, Proc. Roy. Soc. London A180, 333 (1942).

$\text{Bi}^{209}(\text{d},\text{p})\text{Bi}^{210}$ ;  $\text{Bi}^{209}(\text{d},\text{n})\text{Po}^{210}$  - H. E. Tatel and J. M. Cork, Phys. Rev. 71, 159 (1947).

10 Mev:

$\text{Bi}^{209}(\text{d},\text{p})\text{Bi}^{210}$ ;  $\text{Bi}^{209}(\text{d},\text{n})\text{Po}^{210}$  - J. M. Cork, J. Halpern, and H. Tatel,

Phys. Rev. 57, 371 (1940).

$\text{Fe}^{54}(\text{d},\text{n})\text{Co}^{55}$ ;  $\text{Fe}^{54}(\text{d},\alpha)\text{Mn}^{52}$  - J. M. Cork and J. Halpern, Phys. Rev. 57, 667 (1940).

$\text{Ag}^{107}(\text{d},2\text{n})\text{Cd}^{107}$  - D. N. Kundu and M. L. Pool, Bull. Am. Phys. Soc. 25, No. 4,

11 (1950). (Abstract)

11 Mev:

$\text{Be}^9(\text{d},\text{p})\text{Be}^{10}$  - E. M. McMillan, Phys. Rev. 72, 591 (1947).

14 Mev:

$\text{Na}^{23}(\text{d},\text{p})\text{Na}^{24}$ ;  $\text{Br}^{81}(\text{d},\text{p})\text{Br}^{82}$ ;  $\text{Br}^{79}(\text{d},2\text{n})\text{Kr}^{79}$  - E. T. Clarke and J. W. Irvine, Jr.,

Phys. Rev. 66, 231 (1944).

$\text{Mg}^{24}(\text{d},\alpha)\text{Na}^{22}$ ;  $\text{Mg}^{26}(\text{d},\alpha)\text{Na}^{24}$ ;  $\text{Cu}^{63}(\text{d},\text{p})\text{Cu}^{64}$ ;  $\text{Cu}^{65}(\text{d},\alpha)\text{Ni}^{63}$ ;  $\text{Cu}^{63}(\text{d},2\text{n})\text{Zn}^{63}$ ;

$\text{Cu}^{65}(\text{d},2\text{n})\text{Zn}^{65}$  - E. T. Clarke and J. W. Irvine, Jr., Phys. Rev. 69, 680 (1946).

$\text{Al}^{27}(\text{d},\text{p})\text{Na}^{24}$  - E. T. Clarke, Phys. Rev. 71, 187 (1947).

15 Mev:

$\text{Bi}^{209}(\text{d},\text{p})\text{Bi}^{210}$ ;  $\text{Bi}^{209}(\text{d},\text{n})\text{Po}^{210}$  - J. M. Cork, Phys. Rev. 70, 563 (1946).

$\text{Cu}^{63}(\text{d},\text{p})\text{Cu}^{64}$ ;  $\text{Cu}^{63}(\text{d},2\text{n})\text{Zn}^{63}$  - R. S. Livingston and B. T. Wright, Phys. Rev. 58,  
656 (1940).

$\text{Ta}^{181}(\text{d},\text{p})\text{Ta}^{182}$  - Kuan-Han Sun, F. A. Pecjak, R. A. Charpie, J. F. Nechaj,

Phys. Rev. 78, 338 (1950).

19 Mev:

$\text{Bi}^{209}(\text{d},\text{p})\text{RaE}$ ,  $\text{Bi}^{209}(\text{d},\text{n})\text{Po}^{210}$ ,  $\text{Bi}^{209}(\text{d},3\text{n})\text{Po}^{208}$  - E. L. Kelly and E. Segrè,

Phys. Rev. 75, 999 (1949).

$\text{Th}^{232}(\text{d},\text{fiss})$ ;  $\text{U}^{238}(\text{d},\text{fiss})$  - J. Jungerman and S. C. Wright, Phys. Rev. 74,

150 (1948).

190 Mev:

$\text{Al}^{27}(\text{d},\text{ap})\text{Na}^{24}$ ;  $\text{Al}^{27}(\text{d},\text{ap}2\text{n})\text{Na}^{22}$  - A. C. Helmholtz and J. M. Peterson, Phys. Rev.

73, 541 (1948). (Abstract)

$\text{Cu}^{63,65}(\text{d}, )\text{Zn}^{63}$ ;  $\text{Cu}^{63,65}(\text{d}, )\text{Zn}^{62}$ ;  $\text{Cu}^{63,65}(\text{d}, )\text{Ni}$ ;  $\text{Cu}^{63,65}(\text{d}, )\text{Co}$  -

D. Bockhop, A. C. Helmholtz, and J. M. Peterson, Phys. Rev. 74, 1559 (1948).

(Abstract)

$\text{Cu}^{63,65}(\text{d}, )\text{Mn}^{52}$ ;  $\text{Cu}^{63,65}(\text{d}, )\text{Mn}^{56}$ ;  $\text{Cu}^{63,65}(\text{d}, )\text{Fe}^{59}$ ;  $\text{Cu}^{63,65}(\text{d}, )\text{Co}^{56}$ ;

$\text{Cu}^{63,65}(\text{d}, )\text{Zn}^{62}$ ;  $\text{Cu}^{63,65}(\text{d}, )\text{Zn}^{63}$ ;  $\text{Cu}^{63,65}(\text{d}, )\text{Cu}^{64}$  - D. Bockhop, A. C.

Helmholtz, S. D. Softky, J. W. Rose, and T. Breakey, Phys. Rev. 75, 1469 (1949).

(Abstract)

$\text{Cu}^{63,65}(\text{d}, )\text{Mn}^{52}$ ;  $\text{Cu}^{63,65}(\text{d}, )\text{Mn}^{56}$ ;  $\text{Cu}^{63,65}(\text{d}, )\text{Fe}^{52}$ ;  $\text{Cu}^{63,65}(\text{d}, )\text{Fe}^{59}$ ;

$\text{Cu}^{63,65}(\text{d}, )\text{Ni}^{57}$ ;  $\text{Cu}^{65}(\text{d},2\text{p})\text{Ni}^{65}$ ;  $\text{Cu}^{63,65}(\text{d}, )\text{Cu}^{61}$ ;  $\text{Cu}^{63,65}(\text{d}, )\text{Cu}^{64}$ ;

$\text{Cu}^{63,65}(\text{d}, )\text{Zn}^{62}$ ;  $\text{Cu}^{63,65}(\text{d}, )\text{Zn}^{63}$  - F. O. Bartell, A. C. Helmholtz, S. D.

Softky, D. B. Stewart, University of California Radiation Laboratory Unclassified

Report UCRL-757 (July, 1950).

195 Mev:

$\text{C}^{12}(\text{d},\text{dn})\text{C}^{11}$  - R. L. Thornton and R. W. Senseman, Phys. Rev. 72, 872 (1947).

B. Helium Ions5.3 Mev:

$\text{F}^{19}(\alpha,\text{p})\text{Ne}^{22}$ ;  $\text{F}^{19}(\alpha,\text{n})\text{Na}^{22}$  - N. K. Saha, Z. Physik 110, 473 (1938).

$\text{Al}^{27}(\alpha,\text{n})\text{P}^{30}$  - A. Szalay, Nature 141, 972 (1938).

$\text{Al}^{27}(\alpha,\text{n})\text{P}^{30}$  - A. Szalay, Z. Physik 112, 29 (1939).

6 Mev:

$\text{C}^{12}(\alpha,\text{n})\text{N}^{13}$  - W. Riezler, Naturwiss. 34, 157 (1947).

7 Mev:

$\text{Na}^{23}(\alpha,\text{n})\text{Al}^{26}$ ;  $\text{P}^{31}(\alpha,\text{n})\text{Cl}^{34}$  - H. Brandt, Z. Physik 108, 726 (1938).

9 Mev:

$\text{Li}^7(\alpha, n)\text{B}^{10}$  - O. Haxel and E. Stuhlinger, Z. Physik 114, 178 (1939).

$\text{B}(\alpha, n)\text{N}$ ;  $\text{Be}^9(\alpha, n)\text{C}^{12}$  - E. Stuhlinger, Z. Physik 114, 185 (1939).

11 Mev:

$\text{Cu}^{63}(\alpha, n)\text{Ga}^{66}$ ;  $\text{Cu}^{65}(\alpha, n)\text{Ga}^{68}$  - W. B. Mann, Phys. Rev. 52, 405 (1937).

20 Mev:

$\text{Rh}^{103}(\alpha, n)\text{Ag}^{106}$  (25m);  $\text{Rh}^{103}(\alpha, n)\text{Ag}^{106}$  (8.2d);  $\text{Rh}^{103}(\alpha, 2n)\text{Ag}^{105}$  - H. L. Bradt and D. J. Tendam, Phys. Rev. 72, 1117 (1947).

$\text{Ag}^{109}(\alpha, n)\text{In}^{112}$ ;  $\text{Ag}^{109}(\alpha, 2n)\text{In}^{111}$  - D. J. Tendam and H. L. Bradt, Phys. Rev. 72, 1118 (1947).

32 Mev:

$\text{Bi}^{209}(\alpha, 2n)\text{At}^{211}$  - D. R. Corson, K. R. MacKenzie, and E. Segrè, Phys. Rev. 58, 672 (1940).

37 Mev:

$\text{In}^{115}(\alpha, n)\text{Sb}^{118}$ ;  $\text{In}^{115}(\alpha, 2n)\text{Sb}^{117}$ ;  $\text{In}^{115}(\alpha, 3n)\text{Sb}^{116}$  - G. M. Temmer, Phys. Rev. 76, 424, 1002 (1949).

38 Mev:

$\text{Bi}^{209}(\alpha, 2n)\text{At}^{211}$ ;  $\text{Bi}^{209}(\alpha, 3n)\text{At}^{210}$  - E. L. Kelly and E. Segrè, Phys. Rev. 75, 999 (1949).

$\text{Th}^{232}(\alpha, \text{fiss})$ ;  $\text{U}^{238}(\alpha, \text{fiss})$  - J. Jungerman and S. C. Wright, Phys. Rev. 74, 150 (1948).

$\text{Ag}^{107}(\alpha, n)\text{In}^{110}$ ;  $\text{Ag}^{107}(\alpha, 2n)\text{In}^{109}$ ;  $\text{Ag}^{109}(\alpha, 2n)\text{In}^{111}$ ;  $\text{Ag}^{109}(\alpha, 3n)\text{In}^{110}$  -

S. N. Ghoshal, Phys. Rev. 73, 417 (1948).

$\text{Ni}^{60}(\alpha, n)\text{Zn}^{63}$ ;  $\text{Ni}^{60}(\alpha, 2n)\text{Zn}^{62}$ ;  $\text{Ni}^{60}(\alpha, pn)\text{Cu}^{62}$ ;  $\text{Ag}^{107}(\alpha, n)\text{In}^{110}$ ;  $\text{Ag}^{107}(\alpha, 2n)\text{In}^{109}$ ;  $\text{Ag}^{107}(\alpha, 3n)\text{In}^{108}$ ;  $\text{Ag}^{109}(\alpha, 2n)\text{In}^{111}$ ;  $\text{Ag}^{109}(\alpha, 3n)\text{In}^{110}$  - S. N. Ghoshal,

University of California Radiation Laboratory Unclassified Report UCRL-709

Revised (July, 1950).

380 Mev:

$\text{Al}^{27}(\alpha, \alpha 2\text{pn})\text{Na}^{24}$ ;  $\text{Al}^{27}(\alpha, 2\text{an})\text{Na}^{22}$  - A. C. Helmholtz and J. M. Peterson, Phys. Rev. 73, 541 (1948).

390 Mev:

$\text{C}^{12}(\alpha, \text{an})\text{C}^{11}$  - R. L. Thornton and R. W. Senseman, Phys. Rev. 72, 872 (1947).

C. Protons

4 Mev:

$\text{O}^{18}(\text{p}, \text{n})\text{F}^{18}$  - L. A. DuBridge, S. W. Barnes, J. H. Buck, and C. V. Strain, Phys. Rev. 53, 447 (1938).

5 Mev:

$\text{Ag}^{107}(\text{p}, \text{n})\text{Cd}^{107}$  - D. N. Kundu and M. L. Pool, Bull. Am. Phys. Soc. 25, No. 4, 11 (1950). (Abstract)

5.7 Mev:

$\text{N}^{14}(\text{p}, \alpha)\text{C}^{11}$  - W. H. Barkas, Phys. Rev. 56, 287 (1939).

6.6 Mev:

$\text{Cr}^{52}(\text{p}, \text{n})\text{Mn}^{52}$  - A. Hemmendinger, Phys. Rev. 58, 929 (1940).

7 Mev:

$\text{Pd}^{106}(\text{p}, \text{n})\text{Ag}^{106}$ ;  $\text{Pd}(\text{p}, \text{n})\text{Ag}$  (8d + 45d) - T. Enns, Phys. Rev. 56, 872 (1939).  
 $\text{Ni}^{61}(\text{p}, \text{n})\text{Cu}^{61}$ ;  $\text{Ni}^{64}(\text{p}, \text{n})\text{Cu}^{64}$ ;  $\text{Cu}^{63}(\text{p}, \text{n})\text{Zn}^{63}$ ;  $\text{Zn}^{68}(\text{p}, \text{n})\text{Ga}^{68}$ ;  $\text{Pd}^{106}(\text{p}, \text{n})\text{Ag}^{106}$ ;  
 $\text{Ag}^{107}(\text{p}, \text{n})\text{Cd}^{107}$ ;  $\text{Cd}^{114}(\text{p}, \text{n})\text{In}^{114}$  - V. F. Weisskopf and D. H. Ewing, Phys. Rev. 57, 472 (1940).

16 Mev:

$\text{Cu}^{65}(\text{p}, \text{pn})\text{Cu}^{64}$  - J. R. Richardson and B. T. Wright, Phys. Rev. 70, 445 (1946).

32 Mev:

$\text{Cu}^{63}(\text{p},\text{n})\text{Zn}^{63}$ ;  $\text{Cu}^{63}(\text{p},2\text{n})\text{Zn}^{62}$ ;  $\text{Cu}^{63}(\text{p},\text{pn})\text{Cu}^{62}$  - S. N. Ghoshal, University of

California Radiation Laboratory Unclassified Report UCRL-709 Revised (July, 1950).

140 Mev:

Boric acid  $(\text{p}, )\text{C}^{11}$ ;  $\text{C}^{12}(\text{p},\text{pn})\text{C}^{11}$  - W. W. Chupp and E. M. McMillan, Phys. Rev.

72, 873 (1947).

350 Mev:

$\text{C}^{12}(\text{p},\text{pn})\text{C}^{11}$  - Lee Aamodt, Vincent Peterson, and Robert Phillips, Phys. Rev. 78,

87 (1950). (Abstract)